Torrefaction of cellulose, hemicelluloses and lignin extracted from woody and agricultural biomass in TGA-GC/MS: Linking production profiles of volatile species to biomass type and macromolecular composition

María González Martínez, Andrés Anca Couce, Capucine Dupont, Denilson da Silva Perez, Sébastien Thiéry, Xuân-Mi Meyer, Christophe Gourdon

Torrefaction of cellulose, hemicelluloses and lignin extracted from woody and agricultural biomass in TGA-GC/MS: Linking production profiles of volatile species to biomass type and macromolecular composition

María González Martínez [a,*], Andrés Anca Couce [b], Capucine Dupont [c], Denilson da Silva Perez [d], Sébastien Thiéry [e], Xuân-mi Meyer [f], Christophe Gourdon [f]

[a] Université de Toulouse, Mines Albi, CNRS UMR 5302, Centre RAPSODEE, Albi, France
[b] Institute of Thermal Engineering, Graz University of Technology, Inffeldgasse 25b, 8010 Graz, Austria
[c] IHE Delft Institute for Water Education, Department of Environmental Engineering and Water Technology, Delft, The Netherlands
[d] FCBA, InTechFibres Division, Grenoble, France
[e] Université Grenoble Alpes, CEA, Laboratory of Bioresources Preparation (LPB), Grenoble, France
[f] Laboratoire de Génie Chimique, Université de Toulouse, CNRS, INPT, UPS, Toulouse, France

Keywords:
Biomass
Torrefaction
Volatile species
Cellulose
Hemicelluloses
Lignin

A B S T R A C T

The production of volatile species in torrefaction of cellulose, hemicellulose and lignin extracted from woody and agricultural biomass was quantified as a function of temperature. The novel coupling of TGA to GC/MS through a heated storage loop system allowed sampling volatile species released at 11 different temperatures in a single torrefaction experiment between 200 and 300 °C, at 3 °C.min^{-1}. The results showed that the use of extracted fractions obtained from different biomass samples led to the detection of a higher number of species (23) than in previous studies with commercial compounds, obtaining a higher degree of detail in the characterization of the production of volatile species in torrefaction. Volatile species were generally released in this study from lower temperatures than those previously reported for commercial compounds. This may be due to the better preservation of cellulose, hemicellulose and lignin properties in extracted fractions thanks to the optimized extraction procedure. Volatile species production profiles were assessed based on the formation mechanisms proposed in the literature and the production of polysaccharide-based fractions was shown to be correlated to their sugar composition. Finally, production profiles allow identifying the temperature range to enhance the production of a given volatile species in torrefaction.

1. Introduction

Nowadays, there is an increasing awareness on the importance of biomass waste as a renewable source of energy, chemicals and materials. The valorization of underexploited agro- and forest-based biomass resources through thermochemical and biological processes was proposed to this aim (Tamminen et al., 2016). The characteristics of the raw biomass strongly influence the conversion process to be selected, as well as the obtained products. In this work, the fundamentals of biomass torrefaction were studied with a detailed analysis of the torrefaction of the main macromolecular components in lignocellulosic biomass, i.e., cellulose, hemicelluloses and lignin.

1.1. Torrefaction

Torrefaction is a thermochemical conversion process suitable for dry biomass (<60% of moisture). It is typically carried out between 200 and 300 °C, for some minutes to hours, in an oxygen-depleted atmosphere. The torrefied solid product has thermal and processing properties closer to coal and thus is suitable for the replacement of fossil fuels in combustion or gasification (Chen et al., 2021).

Gaseous species released during torrefaction include condensable species, among which the major one is water, and permanent gases, such as CO, CO_2 and CH_4. The proportions of the gaseous products are mainly dependent on torrefaction temperature and residence time, as well as on the feedstock characteristics (W.-H. Chen et al., 2015; L. Chen et al.,

* Corresponding author.
E-mail address: maria.gonzalez_martinez@mines-albi.fr (M. González Martínez).

2015).

Volatile species mostly include fatty acids, phenols, acids, alcohols, furans and ketones (Chih et al., 2019; Ciolkosz and Wallace, 2011; Klinger et al., 2013). The type and amount of volatile species released in torrefaction are mainly conditioned by feedstock characteristics and torrefaction temperature (Chen et al., 2018; González Martínez et al., 2018). In torrefaction, deciduous wood leads to a more significant volatile species release and enhanced solid carbonization compared to coniferous wood (Prins et al., 2006a). Moreover, biomass macromolecular and sugar composition is a key factor determining biomass decomposition pathways and volatile species released through thermochemical conversion (Chen and Kuo, 2011; Collard and Blin, 2014; González Martínez et al., 2018).

At industrial scale, torrefaction gases are usually burned to supply energy to the process, provided their water content and CO_2/CO ratio are low (Bergman et al., 2015). However, previous studies pointed out the interest of recovering certain volatile species released in torrefaction, either as a source of high-added-value products or because of their harmfulness for the process (Lê Thành et al., 2015; Rodriguez Alonso et al., 2016). Currently, condensable species valorization is limited because of the difficulties to characterize and separate the complex volatile species mixture (Detcheberry et al., 2016).

Thermogravimetric analysis (TGA) is a usual technique to study solid evolution through thermochemical conversion at lab-scale (Cheng et al., 2012; Lu et al., 2013; Rodriguez Alonso et al., 2016; Saldarriaga et al., 2015). Gaseous species released in torrefaction are typically analyzed by Fourier Transform Infrared Spectroscopy (FTIR), Gas Chromatography (GC) or High-Performance Liquid Chromatography (HPLC). These analytical methods can be used alone or combined with Flame Ionization Detection (FID) and/or Mass Spectrometry (MS) (Anca-Couce and Obernberger, 2016; Bridgeman et al., 2008; Prins et al., 2006a; Trubetskaya et al., 2021). Permanent gases are analyzed on-line or collected in a gas bag for subsequent analysis (Bates and Ghoniem, 2012). Condensable species are usually collected in cold traps to be then analyzed

Table 1
Origin and proposed mechanism of formation of volatile species in biomass torrefaction.

Chemical compound	Literature			Mechanism	Torrefaction T	Source
	cell	hem	lign			
Acids		**M**		Dehydration, fragmentation and secondary reactions of unstable intermediaries from depolymerization	~ to ↑ T↑ T	(Alén et al., 1996; Hosoya et al., 2007; Peng and Wu, 2010; Prins et al., 2006a; Wang et al., 2016; Werner et al., 2014)(Yang et al., 2007)
	X					
			X	Scission of β-O-4 bonds or of small side chains of the phenylpropane units		(Kuroda and Nakagawa-izumi, 2006)
acetic acid		**M**		Elimination of O-acetyl groups linked to the main xylan chain - 4-O-methylglucuronic acid after elimination of C═O, O-CH_3 (secondary pathway)	~ to ↑ T	(Ponder and Richards, 1991; Shafizadeh et al., 1972)(Shen et al., 2010a)
formic, propionic acid		**M**		Scission of the carboxylic group from the hexuronic acids		(Shen et al., 2010a)
Furans	**M**			Scission of relatively weak linkages by a) direct ring-opening and rearrangement during depolymerization; b) secondary reactions of levoglucosan		(Shen and Gu, 2009)
		M		Depolymerization reactions: - of terminal and lateral elements of xylan chains - of glycosidic linkages between intermediate hemicellulose sugar units - of pyran rings (hexoses), through rearrangement in more stable xylan (pentose) rings	> 220 °C↓ to ↑ T~ to ↑ T~ to ↑ T	(Mundike et al., 2016)(Branca et al., 2013)
furfural	**M**	**M**		a) dehydroxymethylation of the furan ring side chain in 5-HMF; b) rearrangement reactions of 5-HMF		(Shen and Gu, 2009)
Phenols			**M**	Degradation of the β-O-4 bonds, the most common in lignin structure, releasing substituted phenolic compounds close to the original structure of lignin	~ to ↑ T	(Collard and Blin, 2014; Shen et al., 2010c)
	X			rearrangement reactions of 5-HMF and furfural to form aryl compounds		(Shen and Gu, 2009)
		X		Charring of solid residue (methylphenols and phenolic compounds with small substituents)	> 300 °C	(Collard and Blin, 2014; Peng and Wu, 2010)
phenol, guaiacol, syringol			**M**	Degradation of the β-O-4 bonds	↑ T	(Collard and Blin, 2014; Shen et al., 2010c)
vinyl guaiacol			**M**	Degradation of the β-O-4 bonds	~ to ↑ T	(Collard and Blin, 2014; Shen et al., 2010c)
eugenol			**M**			
vanillin			**M**			
Linear ketones	X			Dehydration, fragmentation and secondary reactions of unstable intermediaries from depolymerization	> 280 °C ~ to ↑ T	(Worasuwannarak et al., 2007)
		M				
hydroxyacetone	X			Secondary decomposition of levoglucosan		(Shen and Gu, 2009)
		M		Dehydration, fragmentation and secondary reactions of unstable intermediaries from depolymerization		
			X	From hydroxyl groups from the C- α of the side chain of the phenylpropane unit		(Kuroda and Nakagawa-izumi, 2006)
Cyclic ketones		**M**		Dehydration, fragmentation and secondary reactions of unstable intermediaries from depolymerization	~ to ↑ T	(Alén et al., 1996; Hosoya et al., 2007; Peng and Wu, 2010; Prins et al., 2006a; Wang et al., 2016; Werner et al., 2014)
methanol		**M**		Rupture of methoxy- group of 4-O-methyl-α-D-glucuronic acid		(Prins et al., 2006a)
formaldehyde			**M**	Scission of C-γ of phenylpropane unit with OH and the contiguous C (dehydration)	↓ to ↑ T	(Collard and Blin, 2014; Shen et al., 2010c)
levoglucosan	**M**			Scission of the β-1,4 glycosidic linkage between glucopyranose monomeric units (transglycosylation)	≥ 300	(Scheirs et al., 2001)

X: proposed origin in the literature; **M:** main proposed mechanism.

off-line (Nocquet et al., 2014). However, the main problem of coupling TGA and gas analyzers, such as GC/MS, is the different analysis duration, which limits the number of gaseous samples analyzed per torrefaction experiment (Chen et al., 2020; Zhao et al., 2017).

1.2. Biomass main macromolecular components: thermal degradation

Analyzing biomass decomposition through its main macromolecular components implies studying cellulose, hemicelluloses and lignin degradation pathways. The mechanisms reported in the literature for the formation of the main volatile species in biomass torrefaction as a function of the macromolecular composition were summarized in Table 1. The interactions between these macromolecular components may also impact biomass transformation through thermochemical conversion routes (Chen et al., 2018; Hosoya et al., 2007). However, this is a complex subject of research due to the difficulties in determining and quantifying the nature and influence of cellulose, hemicelluloses and lignin interlinkages. Furthermore, macromolecular components are typically investigated with commercial compounds (Chen et al., 2019; Chen and Kuo, 2011; Nocquet et al., 2014; Zhao et al., 2017), but their representativeness of raw biomass components is controversial.

In this section, the mechanisms of thermal degradation of cellulose, hemicelluloses and lignin are assessed in the torrefaction temperature range. Extractives, ash and other minor components, such as proteins and lipids, were not considered in this study. The low volatilization temperature of most of the extractives suggests a probable release below 200 °C (Lauberts et al., 2018; Moya et al., 2018). In the case of ash, some studies pointed the influence of inorganic elements in biomass thermal degradation (Macedo et al., 2018; Zhang et al., 2018). However, this conclusion remains under discussion, as these studies are typically based on impregnated raw biomass or commercial compounds. Moreover, no link was found between the behavior in torrefaction of biomass samples from the same specie with different inorganic composition (González Martínez et al., 2018).

1.2.1. Cellulose

Cellulose thermal degradation was reported to occur principally between 300 and 400 ºC (Collard and Blin, 2014). In a first step, the intermediate "active cellulose" or "anhydrocellulose" may be formed, depending on the mechanism. "Active cellulose" may be formed through partial depolymerization of cellulose producing levoglucosan, which will be further decomposed into char and volatile species (Lédé, 2012). "Anhydrocellulose" may be resulting from a dehydration reaction producing water, CO and CO_2 (Arseneau, 1971; Piskorz et al., 1986; Scheirs et al., 2001; Mundike et al., 2016). Dehydration reactions occur from low torrefaction temperatures, around 200 °C. Water is the main product released, but CO, CO_2 and small organic compounds are also released from higher temperatures (around 280 °C) (Worasuwannarak et al., 2007). Intermolecular water elimination through hydrogen bonds between two cellulose chains occurs from low torrefaction temperatures and leads to the formation of supplementary covalent bonds. At higher temperatures, intramolecular water from the glucopyranose unit is eliminated, increasing the aromaticity of the solid residue (Scheirs et al., 2001). The main reaction in cellulose depolymerization is transglycosylation, which consists of the scission of the β-1,4 glycosidic linkage between two glucopyranose units (Scheirs et al., 2001). This mechanism starts before 300 ºC and it is enhanced at higher temperatures, producing mainly levoglucosan (or its dehydrated form, levoglucosenone), anhydro-oligosaccharides and anhydro-saccharides. The formation of more stable furan forms from levoglucosan through pyran ring contraction is favored (Wang et al., 2012), which leads to 5-hydroxymethylfurfural (5-HMF), 5-methylfurfural, furfural and furfury alcohol. These compounds can also be produced by direct ring-opening and rearrangement reactions from the depolymerization from cellulose monomers, as well as by the scission of relatively weak linkages. Furfural was reported to be formed thanks to the dehydroxymethylation of the furan ring side chain in 5-HMF. A second proposed route was 5-HMF secondary reactions followed by rearrangements, which also lead to aryl compounds, such as phenol (Shen and Gu, 2009). Depolymerization reactions also produce unstable fragments with carbonyl and carboxyl functions. The dehydration and stabilization reactions of these fragments produce water, CO, CO_2 and low molecular weight organic compounds (hydroxyacetone, hydroxyacetaldehyde and acetaldehyde, among others) (Yang et al., 2007). Hydroxyacetone was also reported to be produced from the direct conversion of cellulose, without the intermediate of levoglucosan (Shen and Gu, 2009).

1.2.2. Hemicelluloses

Hemicellulose thermochemical conversion mostly occurs in the torrefaction temperature range, from around 200–350 ºC, and it is strongly affected by the sugar composition (Werner et al., 2014). Indeed, xylan-based hemicelluloses, principally composing deciduous wood, would be more reactive and more easily degradable than mannan-based hemicelluloses, mainly present in coniferous wood (Prins et al., 2006b). Hemicellulose degradation by dehydration combined with the scission of weak linkages between small substituents and the main polymer chains. This reaction produces methanol when the rupture involves the methoxy- group of the 4-O-methyl-α-D-glucuronic acid (Prins et al., 2006a). However, when the scission concerns the carboxylic group from the hexuronic acids, formic acid is released. A similar mechanism to this latter one was proposed for propionic acid production (Shen et al., 2010a). When temperature increases, the elimination of the O-acetyl groups linked to the main xylan chain is enhanced and leads to the main production of acetic acid (Ponder and Richards, 1991; Shafizadeh et al., 1972). This compound may also be produced from the elimination of the carbonyl and O-methyl groups of the 4-O-methylglucuronic acid after (Shen et al., 2010a). Above 220 ºC, depolymerization starts at the terminal and lateral units of the hemicellulose chains. This mechanism is strongly favored with temperature, as glycosidic linkages become unstable and the scission of intermediate units of the hemicellulose chains also happens (Mundike et al., 2016). Furans, and specially furfural, are directly released from hexose and pentose building blocks from hemicelluloses. Hexose-based sugars, such as glucomannan, can suffer a rearrangement of their pyran rings to more stable xylan rings (Branca et al., 2013). Unstable intermediaries with new chemical functions are also produced, which go through dehydration, fragmentation and secondary reactions, leading to small compounds such as linear ketones (principally hydroxyacetone), cyclopentenones and acetic acid (Alén et al., 1996; Branca et al., 2013; Hosoya et al., 2007; Peng and Wu, 2010; Prins et al., 2006a; Wang et al., 2016; Werner et al., 2014). For temperatures above 300 °C, the formation of methylphenols and other phenolic compounds with small substituents may be derived from charring of the solid residue (Collard and Blin, 2014; Peng and Wu, 2010).

1.2.3. Lignin

Lignin typically follows a progressive and partial degradation during torrefaction, from about 200 °C (Biagini et al., 2006; Williams and Besler, 1996) to high pyrolysis temperatures, around 600–700 °C (W.-H. Chen et al., 2015; L. Chen et al., 2015). Its composition on hydroxyphenyl- (H-), guaiacyl- (G-) and syringyl- (S-) units influences its degradation products in thermochemical conversion. While softwood lignin is principally formed by G- units (90%) and some H- units, hardwood lignin contains varying ratios of G- and S- units. Lignin from herbaceous biomass would be formed by the three types of units (Kirk-Othmer, 1999). Lignin degradation was deeply studied under pyrolysis conditions (del Río et al., 2007, 2005; Ohra-aho et al., 2013, 2005; Zhao et al., 2014). These studies showed that the length and the chemical nature of the substituents of lignin units impact the temperature at which they are released (Kawamoto, 2017). According to this, units containing C═C and C═O structures in side-chain are released at lower temperatures, followed by 2-C-side-chain derivatives, then by units with

short side-chain derivatives (1-C) and finally by the non-substituted lignin units [47]. Under torrefaction conditions, lignin degradation is only partial but starts from around 200 °C. Thus, dehydration reactions through the hydroxyl substituents of the phenolic rings occur from low temperatures. Formaldehyde is released when the hydroxyl group is linked to the C-γ of the phenylpropane unit and the scission occurs between this carbon and the contiguous one. The degradation of the β-O-4 bonds from intermediate torrefaction temperatures produces substituted phenolic compounds close to the original lignin structure (eugenol, isoeugenol, vanillin, vinyl guaiacol) (Collard and Blin, 2014; Shen et al., 2010c). However, according to the literature, phenolic compounds with small side-chains, such as phenol and guaiacol, are rarely produced in torrefaction and might be derived from hemicelluloses. The scission of the β-O-4 bonds, as well as of small side-chains of the phenolic groups, can lead to the release of functional groups as small molecules, such as hydroxyacetone and acetic acid, but in a minor extent than hemicelluloses (Collard and Blin, 2014; Kuroda and Nakagawa-izumi, 2006).

1.3. Objective of this work

The main gaps identified in the literature related to volatile species released in torrefaction are: 1) the use of commercial compounds to represent biomass macromolecular components, which showed its limitations (González Martínez et al., 2021); 2) the absence of studies considering the influence of the biomass type on the behavior of macromolecular components in torrefaction; 3) the limited number of volatile species typically quantified at the same time in torrefaction experiments in dynamic thermal conditions; 4) the difficulty of coupling experimental data and biomass and macromolecular components degradation mechanisms in torrefaction due to the absence of dynamic data in function of temperature.

The objective of this work is to determine volatile species production profiles in torrefaction as a function of temperature, biomass family and macromolecular composition. In this way, it is possible to significantly contribute to explain biomass thermal degradation mechanisms and to identify the most suitable operating conditions for enhancing the production of a given volatile species in torrefaction.

A previous work (González Martínez et al., 2020a) demonstrated that solid mass loss in biomass torrefaction can be more accurately described as the sum of biomass macromolecular components when these are directly extracted from biomass, instead of using commercial compounds. These extracted components were obtained through a sequence of different methods reported in the literature with some in-house adaptations (González Martínez et al., 2020b). This approach considered several biomass samples from different families, as well as different operating conditions than those typically used in the obtention of the corresponding commercial compounds (Chen and Kuo, 2011; Nocquet et al., 2014; Prins et al., 2006a). The present work intends to complement the previous study of solid mass loss by a detailed experimental study on 23 volatile species released in torrefaction from cellulose, hemicellulose and lignin fractions extracted from five woody and agricultural biomass samples.

2. Materials and methods

2.1. Extraction procedure

Biomass macromolecular components were extracted following a sequence of in-house developed methods (Fig. 1) which were deeply described in (González Martínez et al., 2020b, p. 1). Five woody and agricultural biomass samples were treated with this extraction procedure, namely: ash-wood (*Fraxinus* ssp.), beech (*Fagus* ssp.), miscanthus (*Miscanthus* ssp.), pine (*Pinus pinaster*) and wheat straw (*Triticum* ssp.).

Hemicellulose-based fractions are referred to "hemicelluloses 1" (H_1) and "hemicelluloses 2" (H_2). H_1 fraction was obtained through dimethyl sulfoxide (DMSO) extraction, after extractives elimination in ASE (Accelerated Solvent Extractor) with acetone/water and biomass delignification through chlorite. H_2 fraction was obtained through an alkaline treatment of the residue derived from the DMSO extraction.

The residue of the DMSO extraction (DMSOr) contained cellulose and residual hemicellulose sugars. The main cellulose-based fraction, called "cellulose II" (C^{II}), was extracted thanks to an alkaline treatment of DMSOr. The main interest of C^{II} fraction was its high purity, due to its high glucan content and low hemicellulose sugar content. Furthermore, the preservation of amorphous cellulose regions from native cellulose was possible in this fraction thanks to its obtention through cold caustic extraction (González Martínez et al., 2021). On the counterpart, this treatment leads to a mercerization of cellulose, which transformed cellulose allomorphic structure type I, present in DMSOr fraction and native biomass, into cellulose II in C^{II} fraction (Oudiani et al., 2011). In order to consider this change, as well as to study the impact of the presence of hemicellulose sugars on a cellulose fraction, the DMSOr fraction was also characterized and torrefied.

"Lignin" extracted fraction (L) was obtained from extractives free-biomass through a dioxane treatment.

The proposed extraction procedure allowed to obtain five extracted fractions per raw biomass. Polysaccharide-based fractions highlighted in dark blue boxes in Fig. 1 were deeply characterized in terms of monosugar distribution and acetyl group content (Table 2).

2.2. TGA-GC/MS experiments

Torrefaction experiments were carried out in a thermogravimetric analyzer (TGA) coupled with a gas chromatography mass spectrometer device (GC/MS). The coupling was carried out through a 16-loop-heated storage system, which allowed volatile species sampling at several torrefaction temperatures. As a result, solid mass loss, whose results were previously reported in (González Martínez et al., 2020b, p. 1), as well as volatiles species production profiles, can be simultaneously studied versus time and temperature in a single torrefaction experiment.

About 100 mg of sample were loaded in a three-plate crucible (1 cm diameter and 5 mm height per plate, 5 mm distance among plates)

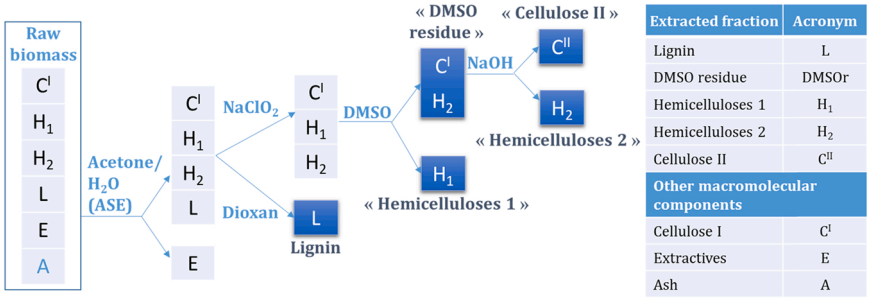

Extracted fraction	Acronym
Lignin	L
DMSO residue	DMSOr
Hemicelluloses 1	H_1
Hemicelluloses 2	H_2
Cellulose II	C^{II}
Other macromolecular components	
Cellulose I	C^I
Extractives	E
Ash	A

Fig. 1. Procedure of extraction of the macromolecular components of biomass (dark blue boxes represent available fractions for characterization and torrefaction, including raw biomass).

Table 2
Neutral monosugar and acetyl groups composition of the sugar-based extracted fractions.

	Extracted fractions composition% of the total monosugars (including acetyl groups)				
	C^{II}				
Monosugars	Ash-wood	Beech	Miscanthus	Pine	Wheat straw
Glucose	98.2	100	100	99.1	100
Xylose	0	0	0	0	0
Mannose	1.8	0	0	0.9	0
Galactose	0	0	0	0	0
Arabinose	0	0	0	0	0
Acetyl groups	n.m.	n.m.	n.m.	n.m.	n.m.
	H_1				
Monosugars	Ash-wood	Beech	Miscanthus	Pine	Wheat straw
Glucose	5.5	0.2	12.5	14.8	32.3
Xylose	72.4	75.9	64.4	18.4	52
Mannose	0	0	0	49.2	0
Galactose	0.3	0.4	0.7	4.1	1.6
Arabinose	0.6	0.6	5.9	3	4.9
Acetyl groups	21.2	22.9	16.5	10.5	9.1
	H_2				
Monosugars	Ash-wood	Beech	Miscanthus	Pine	Wheat straw
Glucose	16.7	12.3	9.8	6.2	9.9
Xylose	75.8	79.9	86.4	80.2	46.6
Mannose	0	0	2	7.5	33.3
Galactose	0.8	0.8	0.6	0.7	3.1
Arabinose	5.8	6.2	0.6	4.2	6.4
Acetyl groups	0.9	0.8	0.7	1.2	0.8
	DMSOr				
Monosugars	Ash-wood	Beech	Miscanthus	Pine	Wheat straw
Glucose	77.3	78.3	76.6	78.7	78.5
Xylose	14.9	16.2	11.9	16.2	5.4
Mannose	1.8	0	5.9	0	11.5
Galactose	0	0	0.2	0	0.2
Arabinose	0.8	0.4	0.3	1.2	0.5
Acetyl groups	5.2	5	5.2	4	3.8

suspended in the TGA (TGA, 92–16.18 SETARAM), reaching a maximum bed thickness of biomass of 0.5 cm per plate. The sample mass was limited to 50 mg for H_1 samples and 25 mg for H_2 samples due to their low density. Samples were torrefied under a 50 mL.min^{-1} helium (He) flow in the thermobalance. This gas was selected due to further GC/MS analysis. The sample was firstly pre-heated from room temperature to 200 ºC, considered as the reference starting temperature, at 3 ºC.min^{-1}. Then, torrefaction was carried out from 200° to 300°C at 3 °C.min^{-1}.

For each experiment, volatile species released during torrefaction were sampled every 10 °C, from 200° to 300°C. As a result, the production profiles of the volatile species were traced (11 points). Gaseous samples were stored at 200 °C in a heated storage loop system (Chromatostock, Antelia), where the gas composition was kept unchanged for at least up to 24 h (Rodriguez Alonso, 2015). A difference exists in the experimental times between torrefaction in TGA (about 60 min) and the analysis in GC/MS of each gaseous fraction collected (70 min). The intermediate heated storage loop system allows multiple sampling of volatile species in a single TGA torrefaction experiment for further analysis in GC/MS.

The chemical composition of each stored volatile fraction was analyzed in GC/MS (Perkin-Elmer Clarus 580/Clarus SQ8S). The GC device consisted of a capillary column Perkin-Elmer Elite-1701 (composition: 14% cyanopropylphenil-85% dimethyl polysiloxane), of 60 m length, 0.25 mm of internal diameter and 0.25 μm of film thickness. The selected non-polar stationary phase is suitable for a large spectrum of chemical species, which fits with the complex nature of the torrefaction gaseous mixture. The injection in the column was direct from the heated storage loop system, by a 1 mL.min^{-1} helium carrier flow that swept the loop and pushed its content in the GC column (splitless injection). The GC temperature program was set as follows: the initial temperature of 45 °C was held 10 min, then the column was heated to 230 °C at 5 °C.min^{-1}, kept at 230 °C during 13.33 min, heated to 250 °C at 5 °C.min^{-1} and kept 250 °C for 5.67 min

MS apparatus was based on an Electron Ionization (EI) ion source, with a range of *m/z* considered from 28 to 300. Chemical species were identified from the chromatogram by using the NIST library. The identification was considered as correct for both Match and RMatch factors higher than 800.

Preliminary experiments confirmed that the selected crucible configuration and experimental conditions ensure chemical regime for all samples (González Martínez et al., 2016). Each torrefaction experiment in TGA-GC/MS was carried out at least twice. The relative error was found to be around 2% for the thermogravimetric analysis and between 15% and 20% for the volatile species quantification. This was considered acceptable because of the small amounts of volatile compounds to be measured.

For a quantitative comparison, production profiles of volatile species were converted from peak areas into an instantaneous mass through calibration. The mass of volatile species produced at each temperature corresponded to an instantaneous production given by the time for filling the sampling loop volume, estimated to 0.5 s. As a result, the mass rate of volatile species released (g.min^{-1}) as a function of time can be represented for each temperature. The integration of the area below this curve for the total duration of each experiment, between 200 and 300 °C, allowed to calculate the total production of a given volatile species in torrefaction. Finally, a mass ratio was calculated at each time and temperature between the mass rate of volatile species released (g.min^{-1}) and the corresponding solid degradation rate (%wmf.min^{-1}), which represented the mass of sample converted. As a result, production profiles of volatile species were represented in g(volatile species released)/g(sample transformed) as a function of time and temperature.

2.3. Volatile species identification

Volatile species were identified by their *m/z* ratio and retention time. Areas below the peaks were quantified in the Extracted Ion Chromatogram (EIC) at the selected *m/z*, to avoid peak overlapping. 51 volatile species were identified in torrefaction experiments (Table 3). They mainly include acids, furans, alcohols, phenols and ketones, which agrees with the literature (Arteaga-Pérez et al., 2015; Chen et al., 2019; Detcheberry et al., 2016; Lê Thành et al., 2015; Nocquet et al., 2014; Prins et al., 2006a; Wang et al., 2012; Werner et al., 2014). 23 of these species were quantified thanks to calibration through standards (Table 3, in bold). Cis- and trans- isoeugenol were considered as a single compound in quantification due to calibration constraints, which may be suitable for a prospective valorization.

The production profiles of the volatile species as a function of time and temperature were represented thanks to the software OriginLab 8.5. The selected method for tracing the curve between experimental points for visualization purposes exclusively was B-spline.

3. Results and discussion

Volatile species production was sampled and quantified from 200° to 300°C, every 10 °C, in a single and continuous torrefaction experiment for each biomass sample, at 3 °C.min^{-1}. In this temperature range, the most relevant degradation phenomena in torrefaction are expected to happen. The total production of volatile species classified by chemical family is firstly presented. Then, the detailed production profiles per volatile species and extracted fraction are discussed.

3.1. Production of volatile species per chemical family

The total production per chemical compound was calculated as an integration of the total production for each volatile species from 200 to 300 ºC. Then, the total mass of all volatile species belonging to the same chemical family (Table 2) was calculated by addition. This operation was carried out for each extracted fraction (Fig. 2).

Table 3
Chemical compounds identified (all) and quantified (in bold) in biomass torrefaction experiments in TGA-GC/MS.

t (min)	Compound name	Family	*m/z*	t (min)	Compound name	Family	*m/z*
3.87	formaldehyde	7 - aldehyde	30	27.82	5-methyl-2-furancarboxaldehyde	2 - furan	110
4.31	methanol	6 - alcohol	31	27.93	1-(acetyloxy)−2-butanone	4 - linear ketone	57
4.75	furan	2 - furan	68	29.09	2(5H)-furanone	2 - furan	55
5.31	acetylformaldehyde	7 - aldehyde	72	29.93	3-methyl-2,5-furandione	2 - furan	68
6.31	2-methylfuran	2 - furan	82	30.18	4H-pyran-4-one	8 - other	96
7.41	2,3-butanedione	4 - linear ketone	86	30.39	2-hydroxy-3-methyl-2-cyclopenten-1-one	5 - cyclic ketone	112
8.10	3-pentanone	4 - linear ketone	57	31.18	3-furancarboxylic acid	1 - acid	112
9.90	formic acid	1 - acid	45	31.36	phenol	3 - phenol	94
11.64	acetic acid	1 - acid	43	32.12	2-methoxyphenol (guaiacol)	3 - phenol	109
12.58	2,3-pentanedione	4 - linear ketone	43	33.62	larixic acid (maltol)	1 - acid	126
13.69	hydroxyacetone	4 - linear ketone	43	33.70	2-hydroxy-gamma-butyrolactone	8 - other	57
14.72	methyl hydroxyacetate	8 - other	31	35.40	levoglucosenone	8 - other	98
17.28	propionic acid	1 - acid	74	35.49	2-methoxy-4-methyl-phenol (creosol)	3 - phenol	95
18.30	2-propenoic acid	1 - acid	72	35.86	Unknown sugar	8 - other	116
19.15	1-hydroxy, 2-butanone	4 - linear ketone	57	38.03	4-ethyl-2-methoxyphenol (ethylguaiacol)	3 - phenol	137
20.75	3-furaldehyde	2 - furan	95	38.96	1,4;3,6-dianhydro-(a)-D-glucopyranose	8 - other	69
22.04	furfural	2 - furan	96	39.73	2-methoxy-4-vinylphenol (vinyl guaiacol)	3 - phenol	150
23.78	2-butenoic acid	1 - acid	86	40.41	eugenol	3 - phenol	164
23.97	2-furanmethanol	2 - furan	98	40.85	cathecol	3 - phenol	110
24.35	1-(acetyloxy)−2-propanone	4 - linear ketone	43	41.18	phenol, 2,6-dimethoxy- (syringol)	3 - phenol	154
24.73	2-butanone	4 - linear ketone	43	41.97	cis-isoeugenol	3 - phenol	164
25.19	acetylfuran	2 - furan	95	43.42	trans-isoeugenol	3 - phenol	164
25.90	4-cyclopentene-1,3-dione	5 - cyclic ketone	96	44.17	vanillin	3 - phenol	151
26.71	1,2-cyclopentanedione	5 - cyclic ketone	98	45.71	P-propylguaiacol	3 - phenol	137
27.03	Ethanone, 1-(3-hydroxy-2-furanyl)- (isomaltol)	5 - cyclic ketone	111	51.90	4-hydroxy-3,5-dimethoxybenzaldehyde	7 - aldehyde	182
27.40	2-furancarboxylic acid, methyl ester	2 - furan	95				

The main torrefaction products from "cellulose II" (C^{II}) fractions were acetic acid and furans, followed by ketones and methanol (Fig. 2A). Phenols were detected in trace amounts, which could come from impurities derived from the extraction procedure. Anhydro-oligosaccharides and anhydro-saccharides, which were reported to be released by cellulose (Ohra-aho et al., 2018; Prins et al., 2006a; Shen et al., 2010b), could not be detected with this set-up, except levoglucosenone. The major volatile species quantified were acetic acid (from 42.2% to 64.3% of the quantified total volatile species production, dependent on the C^{II} fraction), methanol (0.0–14.8%), furfural (9.4–32.0%) and hydroxyacetone (1.0–14.3%). Significant amounts were also detected for 4-cyclopentene-1,3-dione (0.3–6.8%) and 2 (5 H)-furanone (1.3–7.0%).

Acids were the major compounds released from DMSOr fractions (57.0–62.5%), followed by furans, ketones and alcohols (Fig. 2B). Formaldehyde and phenols were detected in trace amounts, below 0.1 mg(volatile specie)/g(DMSOr transformed) for all temperature points. This composition remained relatively close to that obtained for C^{II} fractions. The higher proportion of acetic acid and of volatile species quantified is due to the presence of hemicellulose sugars (Prins et al., 2006a; Werner et al., 2014).

Acids were also the main compounds produced in the torrefaction of all H_1 fractions (58.4–89.1%), followed by furans (3.9–28.7%) and methanol (3.8–10.6%, Fig. 2C). Minor amounts of formaldehyde were also detected, slightly higher for pine and wheat straw H_1 fractions (around 10%). This may correspond to traces of other macromolecular components in the fraction, derived from the extraction procedure. A higher variability in the distribution of the volatile species released per biomass family was found for H_1 fractions compared to cellulose-based fractions (C^{II} and DMSOr), which agreed with their different sugar composition.

The composition of the volatile species of H_2 fractions (Fig. 2D) was different from a typical distribution of hemicellulose products in torrefaction (Fig. 2C). The results showed a lower proportion of acids (17.8–27.1%), due to the removal of the acetyl groups from hemicelluloses in the alkaline treatment (Table 1). This implied an increase in the proportion of methanol and formaldehyde, and, to a minor extent, of furans and ketones.

The major volatile species released per chemical family for L fractions were phenols (23.9–49.9%) and formaldehyde (20.5–51.4%, Fig. 2E). Methanol and acetic acid were also released in significant amounts, while furans and ketones were formed to a minor extent.

These observations agree in general with previous studies in the literature (Arteaga-Pérez et al., 2015; Chen et al., 2021; Collard and Blin, 2014; Lê Thành et al., 2015; Nocquet et al., 2014; Prins et al., 2006a). However, the main advantage is the obtention of production profiles as a function of temperature, presented in the next Section (3.2). In the case of cellulose, the differences in the volatile species detected between extracted cellulose and previous studies based on commercial microcrystalline cellulose may be due to the important structural and chemical differences among these compounds, analyzed in detail in (González Martínez et al., 2021). The main chemical compounds identified in previous studies were quantified here for hemicelluloses, as well as other minor acids, alcohols and ketones (Collard and Blin, 2014). Concerning lignin, phenols and formaldehyde were the main volatile species detected, as expected (Chen et al., 2019; Jakab et al., 1995), while ketones and furans are found to be principally derived from polysaccharides.

3.2. *Production of volatile species per extracted fraction*

In this section, the temperature and time evolution of the production of volatile species are analyzed in detail for each cellulose, hemicellulose and lignin fractions extracted from woody and agricultural biomass. The obtained results lead to a large number of volatile species quantified, from which the most representative ones were selected for discussion. The results obtained for the extracted fractions were compared to previous studies in the literature based on commercial compounds (Nocquet et al., 2014; Zhao et al., 2017). This allowed introducing the effect of the biomass family and its detailed macromolecular composition on the discussion of the volatile species released in torrefaction.

The results of the volatile species production as a function of the biomass type for each extracted fraction are represented in g(volatile species produced)/g(sample transformed). This allows comparing the formation of a volatile species as a function of time and temperature, interdependently of the extent of the degradation and of the biomass type. The degradation rate profiles of each extracted fraction are depicted in Fig. 3, so that the temperature range corresponding to the

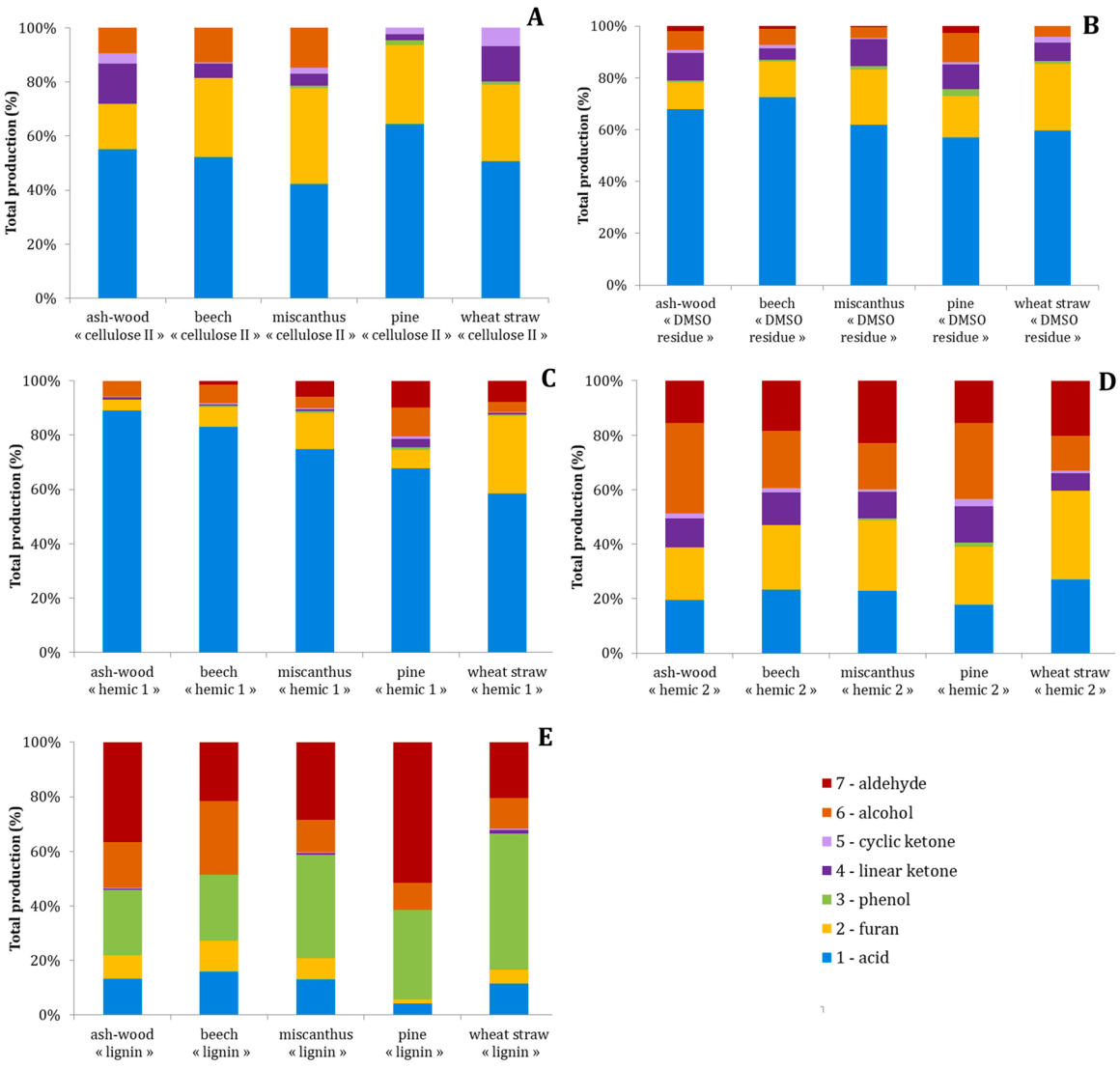

Fig. 2. Distribution of the total production of volatile species per chemical family in torrefaction of the extracted fractions from 5 biomass species in TGA-GC/MS.

main degradation in torrefaction could be identified. The detailed results on the solid transformation through TGA were presented in (González Martínez et al., 2020b, p. 1).

3.2.1. *Cellulose fractions*

3.2.1.1. C^{II} fraction. The production profiles versus temperature of four volatile species quantified in the torrefaction of C^{II} fraction are presented in Fig. 4. In general, similar production profiles were shown for all C^{II} samples for each volatile species. This agreed with their similar sugar composition, based on a high glucose content. Volatile species were detected from low to intermediate torrefaction temperatures, which agreed with solid mass loss profiles (Fig. 4, C^{II}). This highlighted that cellulose degradation might start from lower temperatures (around 220–250 °C) than those previously reported in the literature for commercial compounds (around 280–300 °C) (Shen et al., 2010b). The main reason may be the more preserved structure of C^{II} fractions, compared to that of the commercial microcrystalline cellulose (González Martínez et al., 2021).

Acetic acid was the main quantified compound released in the torrefaction of C^{II} fractions. From 220 °C, its production profile was shown to be independent of the torrefaction temperature (Fig. 4A). In this case, the similar trend for all C^{II} fractions may support that acetic acid is produced from dehydration, fragmentation and secondary reactions of unstable intermediaries in cellulose depolymerization (Shen and Gu, 2009). However, acetic acid was reported to be mainly produced from hemicelluloses degradation. The slightly higher production of acetic acid for ash-wood and pine C^{II} fractions may be related to the presence of residual mannose (< 2%wt, Table 2).

Hydroxyacetone production started from 250° to 260°C for ash-wood and wheat straw C^{II} fractions, followed by an increasing production until 300 °C. For the other C^{II} samples, hydroxyacetone was only produced at 300 °C (Fig. 4B). The decomposition of hydroxyacetone from cellulose degradation may produce formaldehyde and acetaldehyde (Shafizadeh et al., 1972), which were not detected in our case and may be formed at higher temperatures. 2-propanone,1-(acetyloxy)- was also released in a minor amount from 280 °C for all C^{II} fractions.

Furfural was the major furan detected (Fig. 4C). It was reported to be produced by cellulose depolymerization above 300 °C, thanks to the scission of weak bonds liberating furans and levoglucosan (Fred et al., 1979; Shen and Gu, 2009). An increase in the furan yield was reported in the pyrolysis of celluloses with a lowered crystallinity (Wang et al., 2013; Zhang et al., 2010). This might explain the detection of furfural from around 230 °C for all C^{II} fractions, whose crystallinity may be lower than that of the commercial cellulose (González Martínez et al., 2021). Furthermore, furan, acetylfuran and 2(5 H)-furanone started to

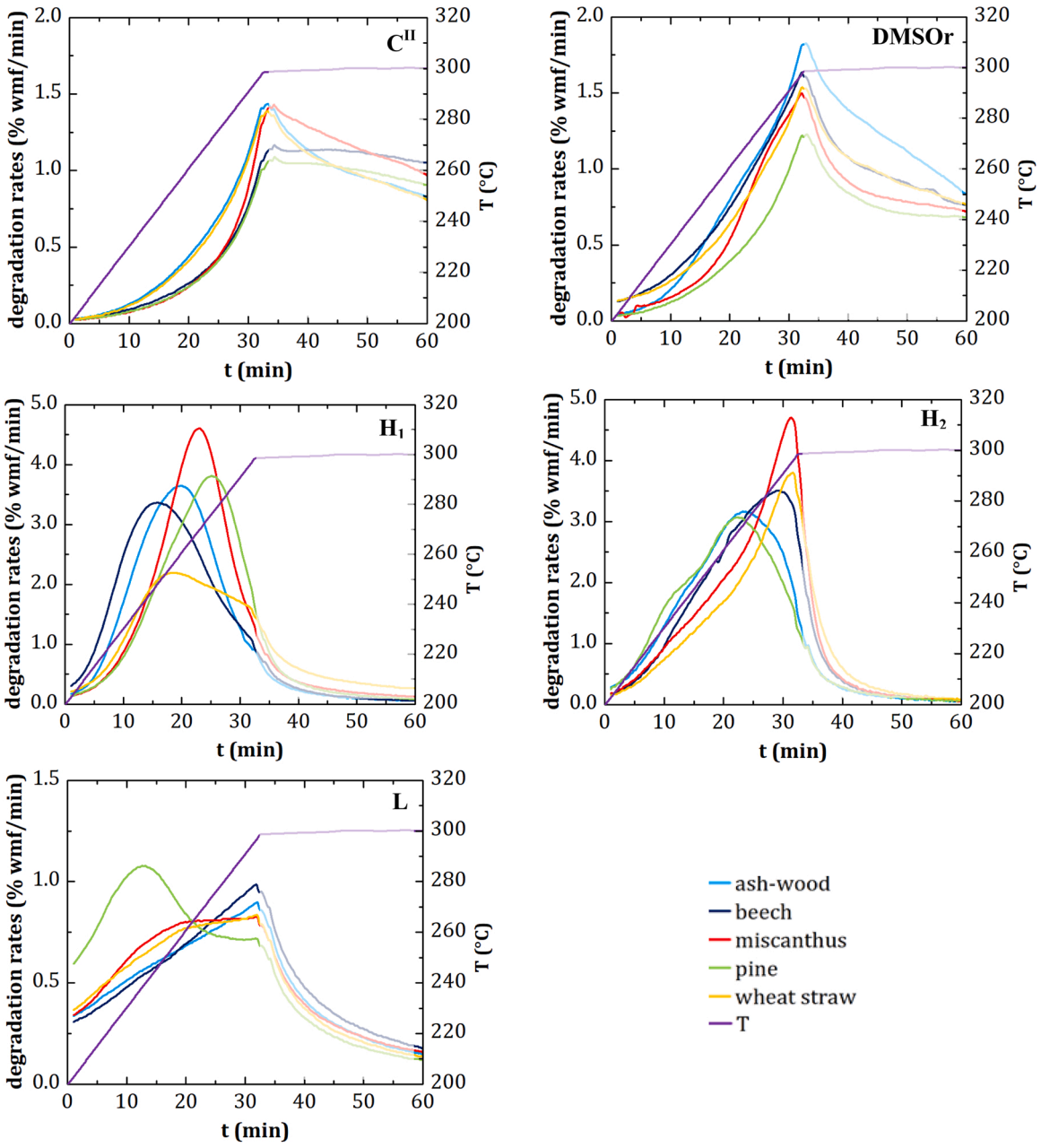

Fig. 3. Degradation rates versus time and temperature in torrefaction in TGA-GC/MS for the extracted fractions ("cellulose II", "DMSO residue", "hemicelluloses 1", "hemicelluloses 2", "lignin") from ash-wood, beech, miscanthus, pine and wheat straw (González Martínez et al., 2020b). The second half of the experiment (isothermal, 300°C) is shadowed as the volatiles were only measured in the first half at 3 °C.min^{-1}, which is the most relevant for torrefaction conditions.

be released from 260° to 280°C. While no trend can be deduced in furan release, acetylfuran and 2(5 H)-furanone (Fig. 4D) showed ascendant profiles of formation, with a local minimum at 290 °C for all C^{II} fractions.

Methanol and 4-cyclopentene-1,3-dione were detected in very low amounts (Figs. 4E and F). They are not typical products from cellulose decomposition. Cyclic ketones are principally produced in hemicellulose depolymerization (Branca et al., 2013; Shen et al., 2010a; Stefanidis et al., 2014). Only rare studies detected cylopentenones in high-temperature pyrolysis of cellulose (Chen et al., 2019; Wu et al., 2009). In this case, the highest production was for wheat straw C^{II}. The absence of hemicellulose residual sugars in this fraction (Table 2) confirms its production from cellulose. Methanol was reported to be principally released in the scission of lignin methoxy groups, as well as of 4-O-methyl-α-D glucuronic acid in hemicelluloses. In our case, this behavior does not seem to be related to residual hemicelluloses. Furthermore, even if residual lignin could not be measured, the severity of chlorite delignification in the extraction procedure should guarantee its complete removal. Some authors suggested that methanol could derive from the secondary decomposition of cellulose anhydrosugars, especially from levoglucosan, rather at high temperatures and long residence time (Shen and Gu, 2009). As observed for other volatile species, the use of extracted celluloses may allow showing this compound from lower temperatures.

3.2.1.2. DMSOr fraction. The volatile species released from the DMSOr fractions in torrefaction were shown to be dependent on biomass origin, mainly due to the strong differences in sugar composition. Furthermore, biomass type may impact the temperature of the maximum production for each chemical compound (Fig. 5).

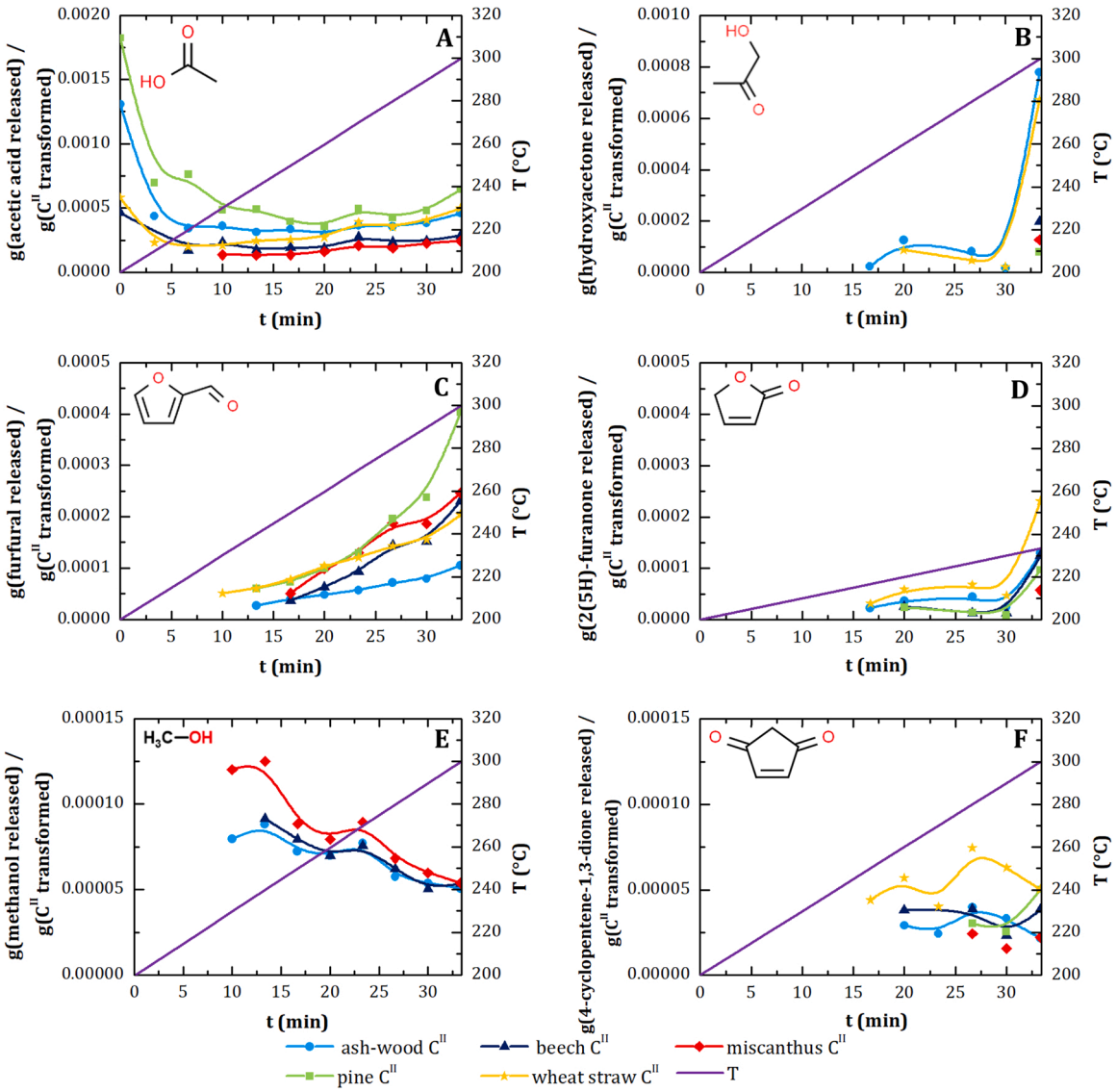

Fig. 4. Production profile versus temperature and time of the major volatile species quantified in the torrefaction of "cellulose II" (C^{II}) fractions in TGA-GC/MS.

Acetic acid was the main quantified compound from DMSOr fractions in torrefaction (Fig. 5A). Its average production remained close to that of the C^{II} fractions. However, its production profile exhibited a maximum of around 250 °C, and at slightly higher temperatures for the pine fraction. This behavior was derived from the presence of hemicellulose sugars in this fraction, which were pointed out as the main source of acetic acid (Chen et al., 2018; Shafizadeh et al., 1972; Werner et al., 2014).

Linear ketones were also detected from lower torrefaction temperatures (Fig. 5B), as for C^{II} fractions. Their production remained the same order of magnitude but it smoothly increased with temperature.

Furans were detected from around 240 °C (Fig. 5C, D). Furfural was detected from lower temperatures than for C^{II} fractions. The production of furans from lower temperatures than those reported (from 300 °C) might respond to the lower crystallinity of cellulose in DMSOr fractions and the presence of hemicellulose sugars. Their production profiles were shown to smoothly increase with torrefaction temperature.

Methanol (Figs. 5E) and 4-cyclopentene-1,3-dione (Fig. 5F) were detected in minor amounts, as in C^{II} fractions. Both compounds exhibited production profiles starting from lower torrefaction temperatures than in the case of the C^{II} fractions, and then decreasing at higher temperatures. Methanol production from DMSOr fractions was slightly higher (Fig. 5E), presumably because of hemicellulose sugars in this fraction.

The comparison of both cellulose-derived fractions, namely C^{II} and DMSOr, highlights the strong influence of the presence of hemicellulose sugars in a cellulose-based fraction. These results showed the relevance of employing C^{II} fraction as representative for the cellulose behavior in torrefaction, instead of using commercial microcrystalline cellulose.

3.2.2. *Hemicellulose fractions*

3.2.2.1. H_1 fraction. The production profiles of the volatile species detected for the H_1 fractions (Fig. 6) were shown to be very dependent on the sugar composition. In some cases, similarities were found for fractions from biomass species from the same family (ash-wood and beech from deciduous wood).

Acetic acid was the main detected compound, accounting from 58.4% of the total volatile species quantified for wheat straw H_1 to 86.7% for the ash-wood H_1. Its production increased with temperature (Fig. 6A) and was an order of magnitude higher than that of C^{II} (Fig. 4A) and DMSOr (Fig. 5A) fractions. The production of acetic acid was related to the fragmentation of acetyl- groups (Prins et al., 2006a) and was described as essentially occurring at the beginning of xylan conversion

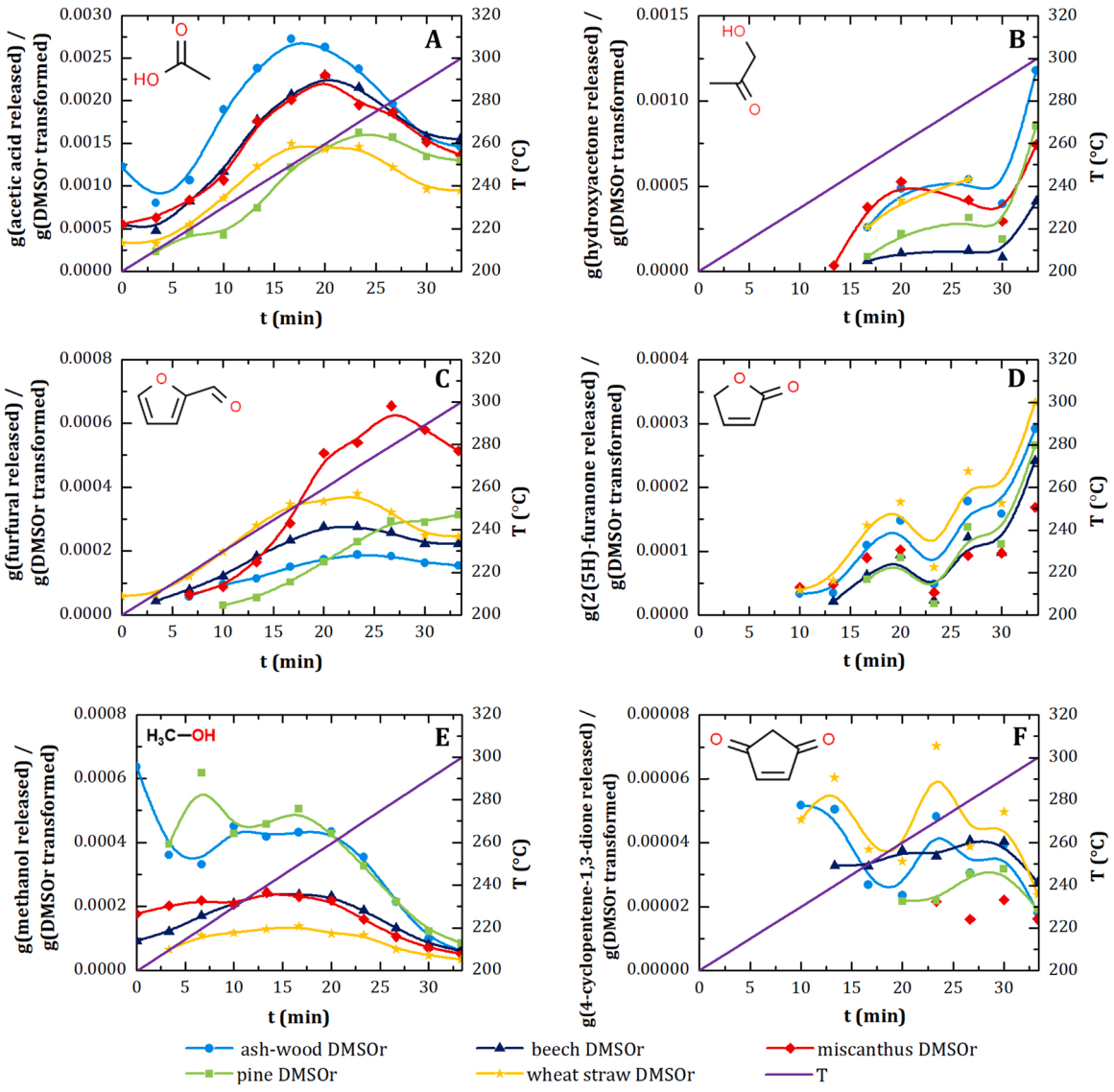

Fig. 5. Production profile versus temperature and time of the major volatile species quantified in the torrefaction of "DMSO residue" (DMSOr) fractions in TGA-GC/MS.

(Collard and Blin, 2014). This agreed with the production detected from low torrefaction temperatures and with the percentage of acetyl groups in H_1 fractions (Table 2).

Pine H_1 fraction led to the higher formic acid production (Fig. 6B), which may be related to its higher mannose content (49.2%). In the literature, the torrefaction of glucomannan-based hemicelluloses was reported to release formic acid. Xylan-based hemicelluloses were reported to be more reactive in torrefaction and to principally release acetic acid (Werner et al., 2014), and formic acid in a minor amount (Nocquet et al., 2014). The maximum formic acid production at 260 °C contrasted with this hypothesis, as acetic acid profiles did not reach a maximum in the torrefaction experiments. This result might be explained by the lower reproducibility achieved for formic acid quantification compared to other compounds. This was mainly due to a low retention time (around 10 min) at which several chromatogram peaks overlapped.

Furfural was detected from low torrefaction temperatures and its production increased with temperature (Fig. 6C). A maximum was found for wheat straw H_1 (around 240 °C), and, to a minor extent, for beech and pine H_1 (220–230 °C). Furfural production was reported to occur from low torrefaction temperatures (Shen et al., 2010a), which is in agreement with the production profiles obtained. However, no evidence was found to explain the maximum observed for three of the profiles. This may be linked to the degree of weakness of the hemicellulose structure due to the extraction procedure and biomass type. Extraction operations may impact in a different extent woody and agricultural samples, leading to differences in the final resistance to thermal degradation of the extracted fractions. This may explain the behavior of wheat straw H_1, as agricultural biomass structure was reported to present a weaker and less complex structure compared to that of woody biomass (Hillis, 1985). The release of furfural was explained through several mechanisms, including ring-open and rearrangement reactions of the xylan (Table 1) (Shen et al., 2010a).

The production profile of other furans follows the example of 2(5H)-furanone (Fig. 6D): a detection from around 240 °C and an increase in production with temperature. Furan, 3-furaldehyde and acetylfuran from pine hemicellulose were detected from 10° to 20°C higher than for hemicelluloses from other biomass species. This might be related to furan production from xylan-based hemicelluloses at lower temperatures (around 240 °C) than from glucomannan-based hemicelluloses (around 270 °C) (Branca et al., 2013; Collard and Blin, 2014; Prins et al., 2006a).

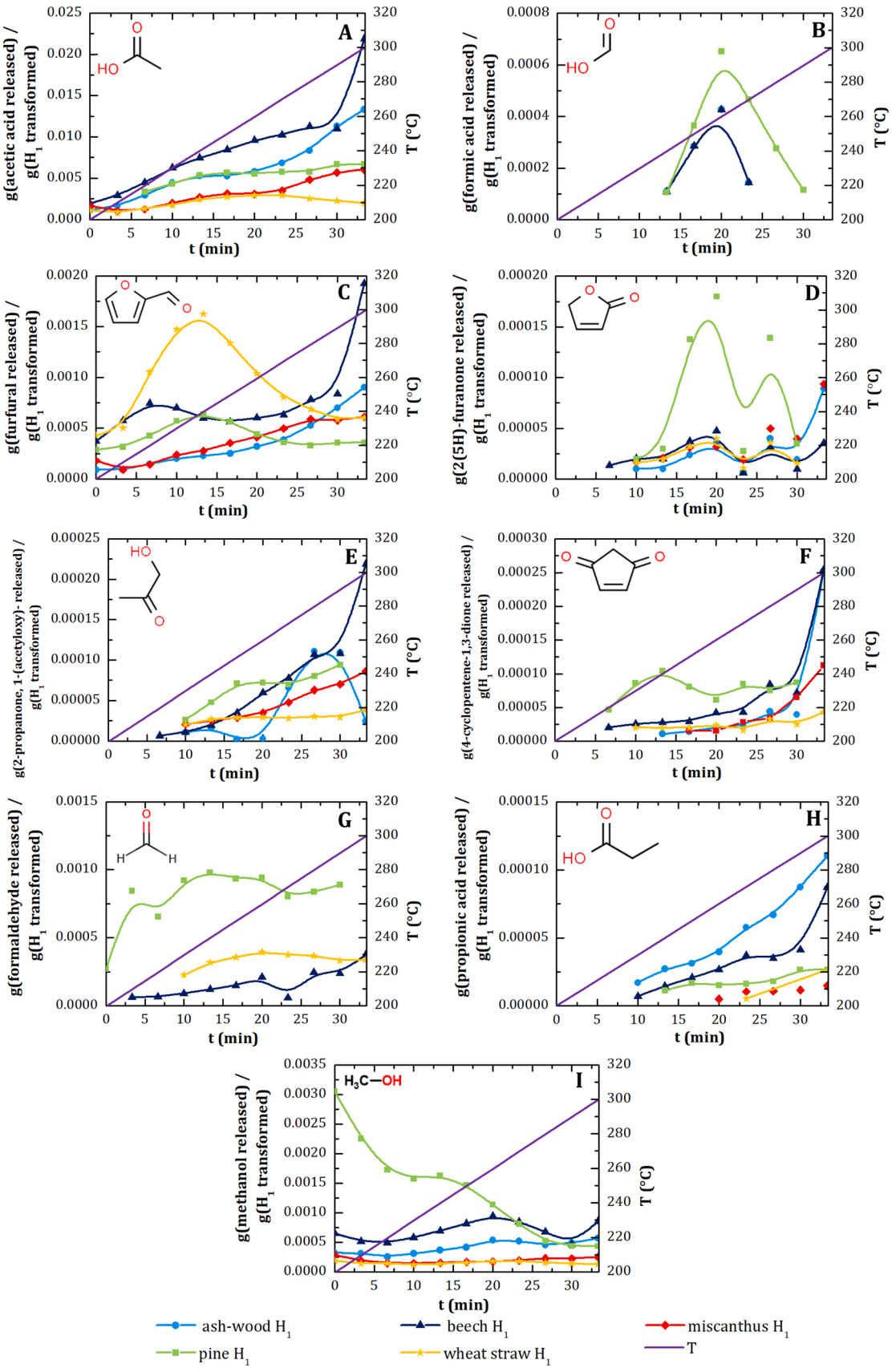

Fig. 6. Production profile versus temperature and time of the major volatile species quantified in the torrefaction of "hemicelluloses 1" (H_1) fractions in TGA-GC/MS.

Linear ketones, including hydroxyacetone and 1-(acetyloxy)−2-propanone, showed production profiles dependent on biomass type. Their production mainly increased with temperature for H_1 from woods, was slightly moderate for miscanthus H_1 and was rather constant for wheat straw H_1 (Fig. 6E). Ketones and other small compounds may come from the rapid depolymerization of hemicelluloses, directly or through dehydration, fragmentation and secondary reactions of unstable intermediates (Table 1). Cyclic ketones can also be formed through this pathway from pyran or furan rings (Fig. 6F) (Collard and Blin, 2014).

Formaldehyde release was significant for pine and wheat straw H_1. Its production was independent of temperature (Fig. 6G). It was reported to be principally released by hydroxymethyl groups (CH_2OH) principally present in lignin and, in a minor extent, in cellulose (Table 1) (Nocquet et al., 2014). Its formation from hemicellulose may thus derive from traces of lignin in the structure or from fragmentation reactions after depolymerization, as for other small molecules.

Propionic acid production was enhanced with temperature for all H_1 fractions (Fig. 6H). It may be derived from the xylan unit with an O-acetyl substituent. However, there is reported a competition of this mechanism with an acetic acid pathway (Shen et al., 2010a). This was

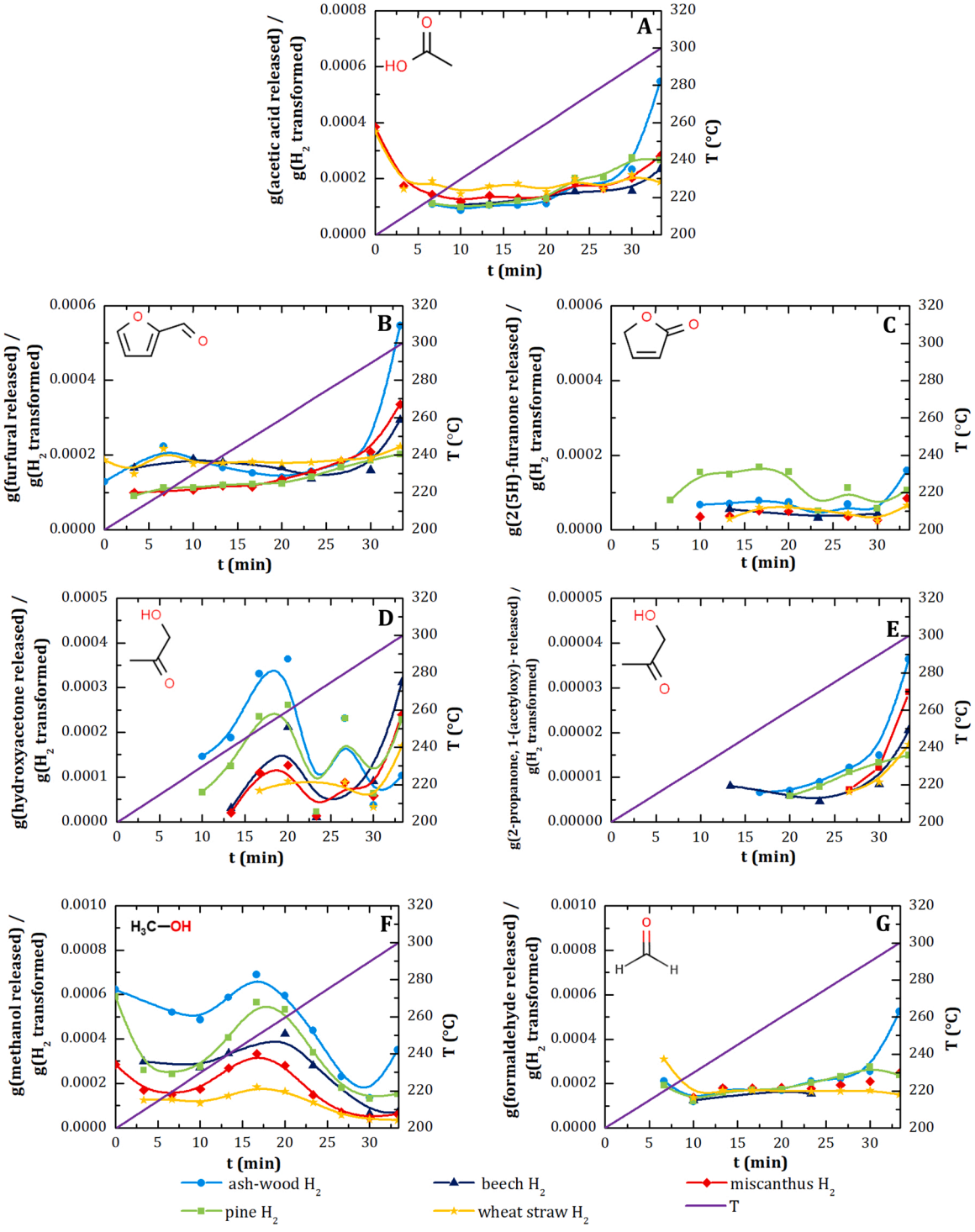

Fig. 7. Production profile versus temperature and time of the major volatile species quantified in the torrefaction of "hemicelluloses 2" (H_2) fractions in TGA-GC/MS.

observed in our study for miscanthus H_1 at high temperatures: while acetic acid production increased, propionic acid production decreased.

Methanol production was shown to be independent of temperature, except for the pine H_1 fraction (Fig. 6I). A local maximum could be seen at intermediate torrefaction temperatures, particularly for deciduous wood for H_1 fractions. Its formation is attributed to the scission of the methoxy- group on C4 position of 4-O-methyl-α-D-glucuronic acid (Shen et al., 2010a), which is a ramification of the xylan chain in hemicellulose structure (Table 1) (Scheller and Ulvskov, 2010). Some studies pointed out that the yield of methanol slightly changes at higher temperatures (above 300 °C), as no competitive reaction consumes the methoxy-groups (Shen et al., 2010a). This mechanism was not observed in our study. The linear decrease in methanol production for pine H_1 may be due to its higher mannose content (Table 2).

Traces of non-substituted lignin-base units, such as guaiacol and syringol, were detected for woody biomass H_1 fractions, while traces of phenol were detected for all H_1 fractions, in all cases below 0.1 mg (volatile species released) / g(H_1 transformed) but with reproducible measurements. In the literature, only vinyl guaiacol was reported to be produced in hemicellulose decomposition at high pyrolysis temperature (Chen et al., 2019). This compound, which was not detected in our study, might be derived from the lignin-like compound ferulic acid, combined with arabinoxylan in some plants (Werner et al., 2014). These traces of phenolic compounds may come from lignin impurities due to the extraction procedure or may be rests of the lignin-carbohydrate complexes (LCC) cross-linking hemicelluloses and lignin (Henriksson et al., 2010).

3.2.2.2. H_2 fraction. H_2 production profiles exhibited similar behavior to those of the H_1 fractions, this is, rather dependent on the sugar composition of the fraction than on the biomass type (Fig. 7). However, for several volatile species, production profiles were shown to be independent of the torrefaction temperature. This behavior might be due to a more degraded structure of H_2 fractions after the alkaline treatment, which facilitated the release of volatile species.

Acetic acid was one of the major compounds detected, with a rather constant production versus temperature (Fig. 7A). This might correspond to small-molecule release during the scission of the sugars from hemicellulose chains and ring-scission between xylose and uronic acid residues (Peng and Wu, 2010; Shen et al., 2010a). Acetyl groups were mostly removed by the alkaline treatment so they were not expected to be the main source of acetic acid (1.0% for H_2; 3.1–22.9% for H_1 fractions; Table 2).

Furfural production profile was independent of temperature (Fig. 7B), which might correspond to rearrangements in xylan structures from low temperatures (Shen et al., 2010a). Higher production rates of furans were detected for glucomannan-based hemicelluloses, namely pine and wheat straw H_2 (7.5% and 33.3% of mannose, respectively). Similarly behaved 2(5 H)-furanone (Fig. 7C).

Linear ketones, namely hydroxyacetone and 1-(acetyloxy)−2-propanone, were detected in higher amounts for H_2 fractions. On the contrary, the production of 4-cyclopentene-1,3-dione was higher for H_1 fractions. However, the production profiles shapes of all ketones were equivalent for both hemicellulose fractions. The production profile of hydroxyacetone showed two marked local minima at 270 and 290 °C for all the H_2 fractions (Fig. 7D). 1-(acetyloxy)−2-propanone production increased with temperature without significant differences among the H_2 fractions (Fig. 7E). No mechanism was found in the literature to explain this point.

Methanol production started from low temperatures for H_2 fractions (Fig. 7F). Then, it remained similar to that of H_1 fractions (Fig. 6I), but it finally decreased close to 300 °C. This behavior might also be derived from a more degraded structure of H_2 fractions.

Formaldehyde production remained at the same order of magnitude for H_1 and H_2 fractions (Figs. 6G and 7G). Both production profiles were rather constant with temperature. This might indicate the same mechanism of formation, probably independent of sugar composition.

3.2.3. L fraction

The production profiles of the volatile species released by L fractions in torrefaction are presented in Fig. 8. For some compounds, similarities were found in the production profiles from agricultural biomass species and herbaceous crops. In the case of woods, the behavior seemed not correlated to biomass family (ash-wood and beech curves). This behavior might be due to the different composition on H-, G- and S- units of lignin for the different biomass types (Kawamoto, 2017).

The major volatile species released from the L fractions was formaldehyde (from 20.5% to 51.4% of the total volatile species quantified). Its production profile was shown to be rather constant during torrefaction (Fig. 8A). This observation agrees with previous studies identifying formaldehyde release from the decomposition of lignin at low temperatures (Nocquet et al., 2014). It may be formed by the scission between Cβ and Cγ of the propyl chain in the lignin structure when the hydroxyl group is linked to the Cγ (Table 1) (Jakab et al., 1995; Liu et al., 2008).

Methanol formation started at low torrefaction temperatures and increased afterward (Fig. 8B) (Nocquet et al., 2014). This compound, together with methane, was reported to be mainly produced in the fragmentation of methoxy- groups linked to aromatic rings from lignin, at temperatures higher than 400 °C (Table 1) (Jakab et al., 1995). As in the previous case, the higher accessibility of extracted lignin might explain its observation from lower temperatures.

Phenols were the main volatile species released in lignin decomposition due to the phenyl propane-based structure of lignin (W.-H. Chen et al., 2015; L. Chen et al., 2015; Kibet et al., 2012; Kirk-Othmer, 1999; Monties, 1980). Substituted-phenolic compounds (i.e. isoeugenol) were released slightly earlier than main lignin units (i.e. guaiacol), which is in agreement with previous results obtained in Py-GC/MS at higher temperatures (González Martínez et al., 2019a). Vinyl guaiacol was the major phenolic compound released, constituting from 4.5% to 22.6% of the total volatile species quantified. This compound, together with eugenol and isoeugenol, showed an enhanced production with torrefaction temperature. This agreed with their proposed mechanisms of formation (Table 1), except for two local minima at 270 °C and 290 °C (Fig. 8D, E, F). At lower temperatures, the α-O-4 (200 °C) and the β-O-4 linkages within monomer units in lignin started to break and liberate phenolic compounds whose structure is close to that of the substituted lignin monomers (Collard and Blin, 2014; Ohra-aho et al., 2013). The production rate of vinyl guaiacol was higher for wheat straw and miscanthus L fractions, compared to woody L fractions (Fig. 8B). The production of isoeugenol was an order of magnitude higher than for eugenol (Fig. 8C). Vanillin showed a constant production profile with temperature (Fig. 8D). Traces of catechol were detected from 260 °C.

The production of phenol, guaiacol and syringol started from around 200 °C and increased with temperature (Fig. 8G, H, I). These compounds, derived from non-substituted H-, G- and S- lignin units, were reported to be released at around 400 °C, through the cleavage of condensed lignin linkages, such a β-1 and β-5 (Kuroda and Nakagawa-izumi, 2006; Kuroda et al., 2007) (Table 1). In our case, they are formed from lower temperatures, probably due to the more accessible structure of L fractions compared to native lignin in biomass. Syringol was not detected for pine lignin, which is in agreement with the absence of S- units on its lignin structure, compared to the other biomass samples, which contain H-, G- and S- units (Monties, 1980).

As polysaccharide-based fractions, L extracted fractions also released acetic acid, but to a lower extent. It might be produced from the scission of the alkyl chains from phenyl units in lignin, together with other small chemical compounds usually up to 3 carbons (Table 1). Acetic acid was detected from around 200 °C, instead of from 300 °C as reported in the literature. As its mechanism of formation seems linked to that of phenolic compounds without alkyl chain, this observation remains

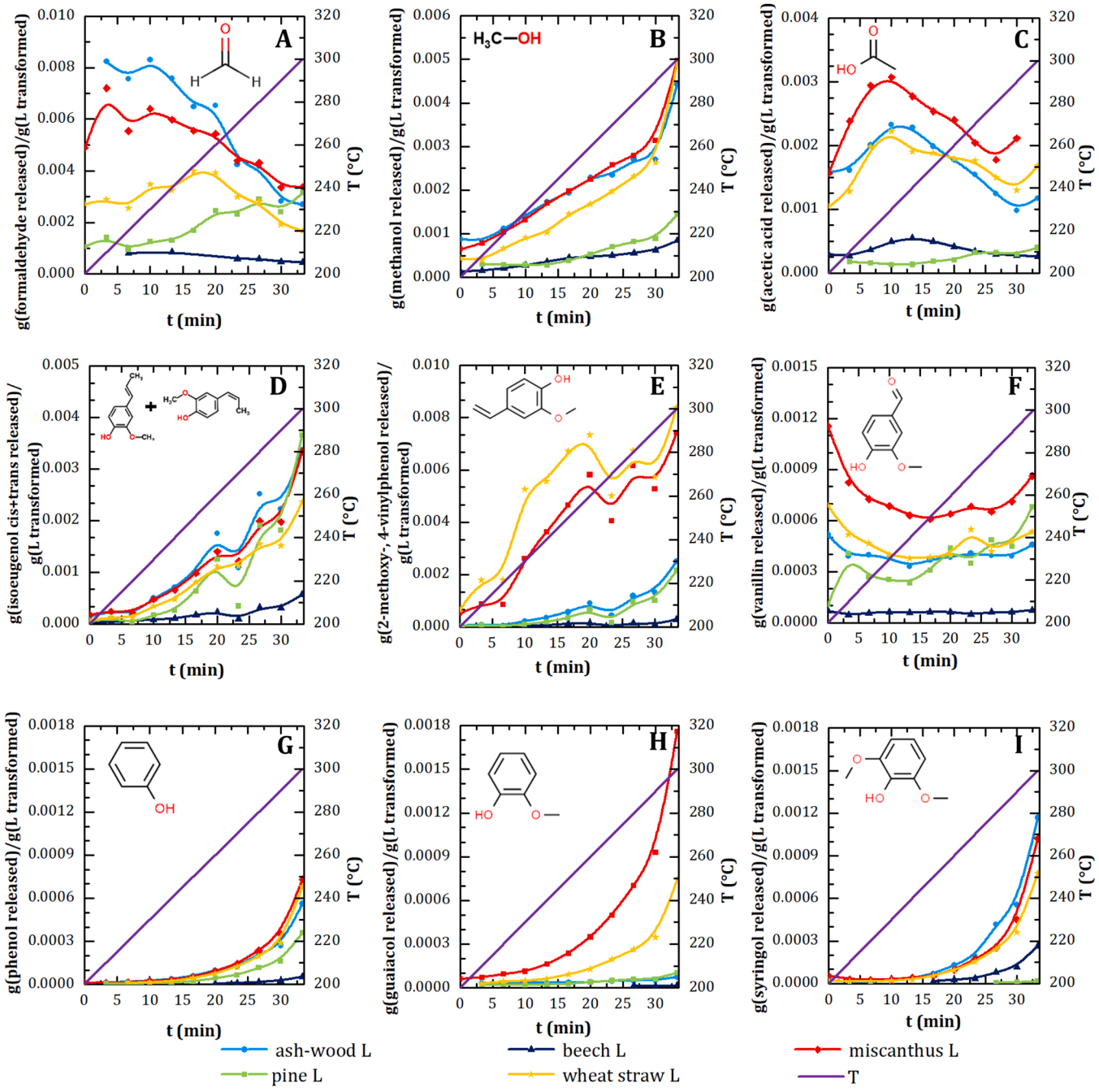

Fig. 8. Production profile versus temperature and time of the major volatile species quantified in the torrefaction of "lignin" (L) fractions in TGA-GC/MS.

consistent with the hypothesis that lignin decomposition might happen since low torrefaction temperatures for lignin extracted fraction. The production profile of acetic acid was constant with torrefaction temperature, as for formaldehyde (Fig. 8C). However, its lower production rate contrasted with the increasing production profiles of small phenolic compounds with temperature. This might indicate that C-C bonds liberating alkyl lateral chains from phenolic compounds might break independently to still be linked to L fractions through α-O-4 and β-O-4 bonds. It would also be the case for the release of methanol from lateral methoxy- groups of phenyl units. This hypothesis supposes the similar stability of this kind of linkages in L fractions.

3.3. *Synthesis of the results*

The results of the volatile species quantified in the torrefaction of the extracted fractions from woody and agricultural biomass species were synthetized in Table 4. These results were compared to those obtained with the same set-up and operating conditions for raw biomass samples (González Martínez et al., 2018).

A higher amount of volatile species was detected and quantified for raw biomass samples compared to the extracted cellulose, hemicellulose and lignin fractions. The number of volatile species identified and quantified for the extracted fractions was higher than that reported in the literature for torrefaction experiments with commercial compounds. Nevertheless, in all cases, the absolute quantified values for the total production per chemical compound and/or extracted fraction were very low. This may be due to a limit of this method related to the real volume of volatile species sampled at each temperature and the technical difficulties to their instantaneous transfer from the heated loops and subsequent injection in the GC/MS for quantification. However, the aim of

Table 4
Quantified volatile species in the torrefaction of cellulose, hemicellulose and lignin extracted based fractions, and of raw biomass samples.

	Extracted fractions					Raw biomass (González Martínez et al., 2018)	Literature		
	C^{II}	DMSOr	H_1	H_2	L		cellulose	hemicelluloses	lignin
Acids	**M**	**M**							
acetic acid	X	X	X	X	X	X		X	
formic acid		X	X	X		X		X	
propionic acid		*	*	*	X	X			
Furans	**M**	**M**							
furan	*	x	X	*	*	X			
3-furaldehyde		*	X	X	*	*			
furfural	X	X	X	X	X	X	X	X	
2-furanmethanol		X	*	*	X	X	X		
acetylfuran	*	*	*		*	*			
2(5H)-furanone	X	X	X	X	*				
Phenols			**M**						
phenol	*	*	*	*	X	X			
2-methoxyphenol (guaiacol)	*	*	*	*	X	X			
vinyl guaiacol					X	X			
eugenol					X	X			X
cathecol					X	X			
2,6-dimethoxyphenol (syringol)			*		X	X			X
isoeugenol (cis+trans)			*		X	X			X
vanillin			*		X	X			
Linear ketones	**M**	**M**							
2,3-pentanedione	*	*	X	*	*	X			
hydroxyacetone	X	x	X	X	*	X	X	X	
1-(acetyloxy)− 2-propanone	X	*	X	*	*	X			
Cyclic ketones		**M**							
4-cyclopentene-1,3-dione	X	*	X	*	*	X		X	
Alcohols									
methanol	X	X	X	X	X	X		X	
Aldehydes									
formaldehyde		X	X	X	X	X			X

X: quantified compound; *: quantified compound in traces ($\leq$ 0.1 mg/g) for all the points of the production profile **M:** main origin of the compound according to literature.

this study is to obtain production profiles of volatile species in biomass torrefaction, and to compare them to the mechanisms proposed in the literature. As a result, these production profiles could be used in further studies as a predictive tool to optimize the production of a given compound versus operating conditions and biomass composition in torrefaction. That is the reason why a relative approach was considered when comparing the production of volatile species per chemical family for a given extracted fraction, as well as for the discussion of the production profiles, for which the main information considered was the shape of the curves.

Some volatile species were released from lower torrefaction temperatures for the extracted fractions than those reported for commercial compounds. Volatile species release for C^{II} fractions starts from 200 °C for acetic acid and around 240 °C for furfural, hydroxyacetone and other compounds, while in the literature cellulose degradation was reported to start around 280–300 °C (Shen et al., 2010b). This might not be related to hemicellulose sugars, as the purity of this fraction in glucose is very high (>98%, Table 2). Acetic acid, furfural and other compounds were released from H_1 and H_2 fractions from around 200 °C, both for xylan and mannan rich hemicelluloses. In the literature, xylan-based hemicelluloses were pointed out as more reactive than mannan-based ones, the degradation of both starting from around 250–270 °C (Prins et al., 2006a). This represents higher temperatures than those observed in our study. As for lignin, significant amounts of substituted phenylpropane units, such as eugenol and vanillin, are detected from 200 °C. This is also observed for non-substituted phenylpropane units, namely phenol, guaiacol and syringol, whose production exponentially increases from around 240 °C. The order of production of these chemical compounds agrees with the literature, but they are also released from lower temperatures than those previously reported (around 400 °C) (González Martínez et al., 2019b; Kawamoto, 2017). The production of volatile species from lower torrefaction temperatures than those identified in the literature may be due to the better accessibility of the extracted fractions compared to macromolecular components in the raw biomass matrix. This may also be due to the closer properties of the extracted fractions to those of macromolecular components in biomass, compared to those of commercial compounds, as discussed in detail for cellulose in (González Martínez et al., 2021). The release of volatile species from lower torrefaction temperatures than those previously reported was already observed for raw biomass samples in torrefaction experiments under identical operating conditions and using the same set-up as in the present study (González Martínez et al., 2018). In the literature, torrefaction experiments with volatile species quantification were typically carried out at a given temperature between 200 °C and 350 °C reached through a heating rate between 5 and 50 °C.min^{-1} (W.-H. W.-H. Chen et al., 2015; L. Chen et al., 2015), instead of under dynamic conditions with intermediate sampling. The slow heating rate selected in our case (3 °C.min^{-1}) may also be the responsible of this behavior. Its aim is to ensure a kinetic regime independent of heat transfer phenomena, which allows comparing the observed production profiles with the suggested mechanisms for biomass torrefaction in the literature.

Inorganic elements may also play a role in the thermal degradation and volatile species release, as reported by some authors in torrefaction (Macedo et al., 2018; Zhang et al., 2018). Extracted fractions inorganic content may be modified compared to that of the raw material, as inorganic elements may be removed during the extraction procedure while others may be added to the fractions due to impurities in chemical products. This may also happen to produce commercial compounds when extracted from biomass, such as beech or birch xylan, but also when they are synthetized, as in both these procedures chemical products are used. According to this, similarities should have to be seen in the behavior of extracted fractions and commercial compounds, which was not the case. Thus, the influence of the inorganic elements at such low temperatures as those corresponding to torrefaction remains unclear according to these results and the literature.

Acetic acid was the major volatile species quantified for all extracted

fractions, except for lignin, mainly releasing formaldehyde. Sugar composition was shown as a determining factor in volatile species release. More precisely, the high purity in glucose of C^{II} fractions leads to a low devolatilization, while the presence of hemicellulose in DMSOr fractions may be the responsible of their devolatilization. The monosugar composition of H_1 and H_2 fractions in xylose, mannose and other minor sugars impacted the composition and the starting temperature of the volatile species produced. L fractions were only partially degraded in the torrefaction temperature range. However, similar results were obtained as those already reported in analytical Py-GC/MS studies at higher temperatures, concerning the release of phenolic derivatives equivalent to substituted lignin units (eugenol, vinyl guaiacol) at lower temperatures than the equivalent non-substituted compounds (phenol, guaiacol) (del Río et al., 2007; González Martínez et al., 2019b). The volatile species released by L fractions agreed with the composition on H-, G- and S- units of raw biomass previously reported (del Río et al., 2007). These results highlight the importance of considering biomass samples from different families (deciduous and coniferous woods, herbaceous crops, agricultural biomasses) to study volatile species release in biomass torrefaction.

4. Conclusions

The production profiles of the volatile species released from biomass macromolecular components in torrefaction as a function of the temperature, in chemical kinetic regime conditions, contributed to a better understanding of the mechanisms involved in the decomposition of cellulose, hemicelluloses and lignin in torrefaction.

Biomass diversity was shown to impact the formation of volatile species through torrefaction, even for biomass species that are biologically close. Furthermore, the properties of biomass macromolecular components, in particular the sugar composition, strongly impact their behavior in torrefaction. As a result, biomass type and macromolecular composition appear as key parameters to be considered when describing biomass behavior in torrefaction in terms of volatile species release, as it was already the case for solid mass loss kinetics (González Martínez et al., 2020b).

The use of extracted macromolecular components instead of commercial compounds leads to a higher number of volatile species released. Moreover, these compounds are generally released from lower temperatures than those reported in the literature in torrefaction experiments with commercial compounds. A reason for this behavior might be the closer characteristics of the extracted fractions to those of macromolecular components in biomass, particularly in terms of sugar composition of the polysaccharide-based fractions, while commercial compounds properties are considerably different. Furthermore, the better accessibility of the extracted cellulose, hemicelluloses and lignin fractions, compared to that of macromolecular components in the raw biomass matrix, can also play a role in it. Finally, the slow heating rate selected for observing volatile species release in biomass torrefaction can contribute to this phenomenon, which was already partly observed in raw biomass torrefaction under identical conditions.

The obtained production profiles may contribute to identify the optimal biomass composition and temperature to enhance the production in torrefaction of a targeted chemical compound among the gaseous species released. Furthermore, the large number of volatile species quantified for different biomass types constitutes a suitable database for modelling volatile species release in torrefaction in future work.

CRediT authorship contribution statement

María González Martínez: Conceptualization, Investigation, Formal analysis, Methodology, Visualization, Writing – original draft, Writing – review & editing. **Andrés Anca Couce:** Formal analysis, Visualization, Writing – review & editing. **Capucine Dupont:** Conceptualization, Supervision, Project administration, Funding acquisition. **Denilson da Silva Perez:** Conceptualization, Methodology, Resources, Investigation. **Sébastien Thiéry**: Investigation. **Xuân-mi Meyer:** Methodology, Supervision, Validation. **Christophe Gourdon:** Methodology, Supervision, Validation.

Declaration of Competing Interest

The authors declare that they have no known competing financial interests or personal relationships that could have appeared to influence the work reported in this paper.

Acknowledgments

This project has received funding from the European Union's Horizon 2020 Research and Innovation Program under grant agreement No 637020-MOBILE FLIP. The Université Fédérale de Toulouse Midi-Pyrénées (France), CEA-LITEN and FCBA (Grenoble, France) are also acknowledged for the support of this work.

References

Alén, R., Kuoppala, E., Oesch, P., 1996. Formation of the main degradation compound groups from wood and its components during pyrolysis. J. Anal. Appl. Pyrolysis 36, 137–148. https://doi.org/10.1016/0165-2370(96)00932-1.

Anca-Couce, A., Obernberger, I., 2016. Application of a detailed biomass pyrolysis kinetic scheme to hardwood and softwood torrefaction. Fuel 167, 158–167. https://doi.org/10.1016/j.fuel.2015.11.062.

Arseneau, D.F., 1971. Competitive reactions in the thermal decomposition of cellulose. Can. J. Chem. 49, 632–638. https://doi.org/10.1139/v71-101.

Arteaga-Pérez, L.E., Segura, C., Bustamante-García, V., Gómez Cápiro, O., Jiménez, R., 2015. Torrefaction of wood and bark from Eucalyptus globulus and Eucalyptus nitens: Focus on volatile evolution vs feasible temperatures. Energy 93 (2), 1731–1741. https://doi.org/10.1016/j.energy.2015.10.007.

Bates, R.B., Ghoniem, A.F., 2012. Biomass torrefaction: modeling of volatile and solid product evolution kinetics. Bioresour. Technol. 124, 460–469. https://doi.org/10.1016/j.biortech.2012.07.018.

Bergman, P.C.A., Boersma, A.R., Zwart, R.W.R., Kiel, J.H.A., 2015. Torrefaction for biomass co-firing in existing coal-fired power stations "BIOCOAL" (No. ECN-C-05–013). Energy research Centre of the Netherlands (ECN).

Biagini, E., Barontini, F., Tognotti, L., 2006. Devolatilization of biomass fuels and biomass components studied by TG/FTIR technique. Ind. Eng. Chem. Res. 45, 4486–4493. https://doi.org/10.1021/ie0514049.

Branca, C., Blasi, C.D., Mango, C., Hrablay, I., 2013. Products and Kinetics of Glucomannan Pyrolysis [WWW Document]. https://doi.org/10.1021/ie400155x.

Bridgeman, T.G., Jones, J.M., Shield, I., Williams, P.T., 2008. Torrefaction of reed canary grass, wheat straw and willow to enhance solid fuel qualities and combustion properties. Fuel 87, 844–856. https://doi.org/10.1016/j.fuel.2007.05.041.

Chen, D., Chen, F., Cen, K., Cao, X., Zhang, J., Zhou, J., 2020. Upgrading rice husk via oxidative torrefaction: characterization of solid, liquid, gaseous products and a comparison with non-oxidative torrefaction. Fuel 275, 117936. https://doi.org/10.1016/j.fuel.2020.117936.

Chen, D., Gao, A., Cen, K., Zhang, J., Cao, X., Ma, Z., 2018. Investigation of biomass torrefaction based on three major components: hemicellulose, cellulose, and lignin. Energy Convers. Manag. 169, 228–237. https://doi.org/10.1016/j.enconman.2018.05.063.

Chen, L., Wang, X., Yang, H., Lu, Q., Li, D., Yang, Q., Chen, H., 2015. Study on pyrolysis behaviors of non-woody lignins with TG-FTIR and Py-GC/MS. J. Anal. Appl. Pyrolysis 113, 499–507. https://doi.org/10.1016/j.jaap.2015.03.018.

Chen, W.-H., Kuo, P.-C., 2011. Isothermal torrefaction kinetics of hemicellulose, cellulose, lignin and xylan using thermogravimetric analysis. Energy 36, 6451–6460. https://doi.org/10.1016/j.energy.2011.09.022.

Chen, W.-H., Lin, B.-J., Lin, Y.-Y., Chu, Y.-S., Ubando, A.T., Show, P.L., Ong, H.C., Chang, J.-S., Ho, S.-H., Culaba, A.B., Pétrissans, A., Pétrissans, M., 2021. Progress in biomass torrefaction: principles, applications and challenges. Prog. Energy Combust. Sci. 82, 100887 https://doi.org/10.1016/j.pecs.2020.100887.

Chen, W.-H., Peng, J., Bi, X.T., 2015. A state-of-the-art review of biomass torrefaction, densification and applications. Renew. Sustain. Energy Rev. 44, 847–866. https://doi.org/10.1016/j.rser.2014.12.039.

Chen, W.-H., Wang, C.-W., Ong, H.C., Show, P.L., Hsieh, T.-H., 2019. Torrefaction, pyrolysis and two-stage thermodegradation of hemicellulose, cellulose and lignin. Fuel 258, 116168. https://doi.org/10.1016/j.fuel.2019.116168.

Cheng, K., Winter, W.T., Stipanovic, A.J., 2012. A modulated-TGA approach to the kinetics of lignocellulosic biomass pyrolysis/combustion. Polym. Degrad. Stab. 97, 1606–1615. https://doi.org/10.1016/j.polymdegradstab.2012.06.027.

Chih, Y.-K., Chen, W.-H., Ong, H.C., Show, P.L., 2019. Product characteristics of torrefied wood sawdust in normal and vacuum environments. Energies 12, 3844. https://doi.org/10.3390/en12203844.

Ciolkosz, D., Wallace, R., 2011. A review of torrefaction for bioenergy feedstock production. Biofuels Bioprod. Bioref. 5, 317–329. https://doi.org/10.1002/bbb.275.

Collard, F.-X., Blin, J., 2014. A review on pyrolysis of biomass constituents: Mechanisms and composition of the products obtained from the conversion of cellulose, hemicelluloses and lignin. Renew. Sustain. Energy Rev. 38, 594–608. https://doi.org/10.1016/j.rser.2014.06.013.

del Río, J.C., Gutiérrez, A., Hernando, M., Landín, P., Romero, J., Martínez, Á.T., 2005. Determining the influence of eucalypt lignin composition in paper pulp yield using Py-GC/MS. J. Anal. Appl. Pyrolysis, Pyrolysis 2004 (74), 110–115. https://doi.org/10.1016/j.jaap.2004.10.010.

del Río, J.C., Gutiérrez, A., Rodríguez, I.M., Ibarra, D., Martínez, Á.T., 2007. Composition of non-woody plant lignins and cinnamic acids by Py-GC/MS, Py/TMAH and FT-IR. J. Anal. Appl. Pyrolysis, PYROLYSIS 2006: Papers presented at the 17th International Symposium on Analytical and Applied Pyrolysis, Budapest, Hungary, 22–26 May 2006 79, 39–46. https://doi.org/10.1016/j.jaap.2006.09.003.

Detcheberry, M., Destrac, P., Massebeuf, S., Baudouin, O., Gerbaud, V., Condoret, J.-S., Meyer, X.-M., 2016. Thermodynamic modeling of the condensable fraction of a gaseous effluent from lignocellulosic biomass torrefaction. Fluid Ph. Equilib. 409, 242–255. https://doi.org/10.1016/j.fluid.2015.09.025.

Fred, S., F.R, H., C.T, G., S.J, P., Yoshio, S., 1979. Production of levoglucosan and glucose from pyrolysis of cellulosic materials. J. Appl. Polym. Sci. 23, 3525–3539. https://doi.org/10.1002/app.1979.070231209.

González Martínez, M., Dupont, C., Anca-Couce, A., da Silva Perez, D., Boissonnet, G., Thiéry, S., Meyer, X., Gourdon, C., 2020a. Understanding the torrefaction of woody and agricultural biomasses through their extracted macromolecular components. Part 2: torrefaction model. Energy 210, 118451. https://doi.org/10.1016/j.energy.2020.118451.

González Martínez, M., Dupont, C., da Silva Perez, D., Mortha, G., Thiéry, S., Meyer, X., Gourdon, C., 2020b. Understanding the torrefaction of woody and agricultural biomasses through their extracted macromolecular components. Part 1: experimental thermogravimetric solid mass loss. Energy 205, 118067. https://doi.org/10.1016/j.energy.2020.118067.

González Martínez, M., Dupont, C., Thiéry, S., Meyer, X.-M., Gourdon, C., 2018. Impact of biomass diversity on torrefaction: study of solid conversion and volatile species formation through an innovative TGA-GC/MS apparatus. Biomass Bioenergy 119, 43–53. https://doi.org/10.1016/j.biombioe.2018.09.002.

González Martínez, M., Dupont, C., Thiery, S., Meyer, X.M., Gourdon, C., 2016. Characteristic time analysis of biomass torrefaction phenomena - application to thermogravimetric analysis device. Chem. Eng. Trans. 50, 61–66. https://doi.org/10.3303/CET1650011.

González Martínez, M., Marlin, N., Da Silva Perez, D., Dupont, C., del Mar Saavedra Rios, C., Meyer, X.-M., Gourdon, C., Mortha, G., 2021. Impact of cellulose properties on its behavior in torrefaction: commercial microcrystalline cellulose versus cotton linters and celluloses extracted from woody and agricultural biomass. Cellulose. https://doi.org/10.1007/s10570-021-03812-y.

González Martínez, M., Ohra-aho, T., da Silva Perez, D., Tamminen, T., Dupont, C., 2019a. Influence of step duration in fractionated Py-GC/MS of lignocellulosic biomass. J. Anal. Appl. Pyrolysis 137, 195–202. https://doi.org/10.1016/j.jaap.2018.11.026.

González Martínez, M., Ohra-aho, T., Tamminen, T., da Silva Perez, D., Campargue, M., Dupont, C., 2019b. Detailed structural elucidation of different lignocellulosic biomass types using optimized temperature and time profiles in fractionated Py-GC/MS. J. Anal. Appl. Pyrolysis 140, 112–124. https://doi.org/10.1016/j.jaap.2019.02.011.

Henriksson, G., Li, J., Zhang, L., Lindström, M.E., 2010. Chapter 9: lignin utilization. Thermochem. Convers. Biomass. Liq. Fuels Chem.

Hillis, W.E., 1985. Wood and biomass ultrastructure. In: Overend, R.P., Milne, T.A., Mudge, L.K. (Eds.), Fundamentals of Thermochemical Biomass Conversion. Springer, Netherlands, Dordrecht, pp. 1–33. https://doi.org/10.1007/978-94-009-4932-4_1.

Hosoya, T., Kawamoto, H., Saka, S., 2007. Cellulose–hemicellulose and cellulose–lignin interactions in wood pyrolysis at gasification temperature. J. Anal. Appl. Pyrolysis 80, 118–125. https://doi.org/10.1016/j.jaap.2007.01.006.

Jakab, E., Faix, O., Till, F., Székely, T., 1995. Thermogravimetry/mass spectrometry study of six lignins within the scope of an international round robin test. J. Anal. Appl. Pyrolysis 35, 167–179. https://doi.org/10.1016/0165-2370(95)00907-7.

Kawamoto, H., 2017. Lignin pyrolysis reactions. J. Wood Sci. 63, 117–132. https://doi.org/10.1007/s10086-016-1606-z.

Kibet, J., Khachatryan, L., Dellinger, B., 2012. Molecular products and radicals from pyrolysis of lignin. Environ. Sci. Technol. 46, 12994–13001. https://doi.org/10.1021/es302942c.

Kirk-Othmer, 1999. Encyclopedia of Chemical Technology. Willey.

Klinger, J., Bar-Ziv, E., Shonnard, D., 2013. Kinetic study of aspen during torrefaction. J. Anal. Appl. Pyrolysis 104, 146–152. https://doi.org/10.1016/j.jaap.2013.08.010.

Kuroda, K., Nakagawa-izumi, A., 2006. Analytical pyrolysis of lignin: Products stemming from β-5 substructures. Org. Geochem. 37, 665–673. https://doi.org/10.1016/j.orggeochem.2006.01.012.

Kuroda, K.-I., Ashitani, T., Fujita, K., Hattori, T., 2007. Thermal behavior of beta-1 subunits in lignin: pyrolysis of 1,2-diarylpropane-1,3-diol-type lignin model compounds. J. Agric. Food Chem. 55, 2770–2778. https://doi.org/10.1021/jf0628126.

Lauberts, M., Lauberte, L., Arshanitsa, A., Dizhbite, T., Dobele, G., Bikovens, O., Telysheva, G., 2018. Structural transformations of wood and cereal biomass components induced by microwave assisted torrefaction with emphasis on extractable value chemicals obtaining. J. Anal. Appl. Pyrolysis. https://doi.org/10.1016/j.jaap.2018.03.025.

Lê Thành, K., Commandré, J.-M., Valette, J., Volle, G., Meyer, M., 2015. Detailed identification and quantification of the condensable species released during torrefaction of lignocellulosic biomasses. Fuel Process. Technol. 139, 226–235. https://doi.org/10.1016/j.fuproc.2015.07.001.

Lédé, J., 2012. Cellulose pyrolysis kinetics: an historical review on the existence and role of intermediate active cellulose. J. Anal. Appl. Pyrolysis 94, 17–32. https://doi.org/10.1016/j.jaap.2011.12.019.

Liu, Q., Wang, S., Zheng, Y., Luo, Z., Cen, K., 2008. Mechanism study of wood lignin pyrolysis by using TG–FTIR analysis. J. Anal. Appl. Pyrolysis 82, 170–177. https://doi.org/10.1016/j.jaap.2008.03.007.

Lu, K.-M., Lee, W.-J., Chen, W.-H., Lin, T.-C., 2013. Thermogravimetric analysis and kinetics of co-pyrolysis of raw/torrefied wood and coal blends. Appl. Energy 105, 57–65. https://doi.org/10.1016/j.apenergy.2012.12.050.

Macedo, L.A., de, Commandré, J.-M., Rousset, P., Valette, J., Pétrissans, M., 2018. Influence of potassium carbonate addition on the condensable species released during wood torrefaction. Fuel Process. Technol. 169, 248–257. https://doi.org/10.1016/j.fuproc.2017.10.012.

Monties, B., 1980. Les polymères végetaux: les lignines. Biochim. Appl.

Moya, R., Rodríguez-Zúñiga, A., Puente-Urbina, A., Gaitán-Álvarez, J., 2018. Study of light, middle and severe torrefaction and effects of extractives and chemical compositions on torrefaction process by thermogravimetric analysis in five fast-growing plantations of Costa Rica. Energy 149, 1–10. https://doi.org/10.1016/j.energy.2018.02.049.

Mundike, J., Collard, F.-X., Görgens, J.F., 2016. Torrefaction of invasive alien plants: influence of heating rate and other conversion parameters on mass yield and higher heating value. Bioresour. Technol. 209, 90–99. https://doi.org/10.1016/j.biortech.2016.02.082.

Nocquet, T., Dupont, C., Commandre, J.-M., Grateau, M., Thiery, S., Salvador, S., 2014. Volatile species release during torrefaction of wood and its macromolecular constituents: Part 1 – experimental study. Energy 72, 180–187. https://doi.org/10.1016/j.energy.2014.02.061.

Ohra-aho, T., Gomes, F.J.B., Colodette, J.L., Tamminen, T., 2018. Carbohydrate composition in Eucalyptus wood and pulps – comparison between Py-GC/MS and acid hydrolysis. J. Anal. Appl. Pyrolysis 129, 215–220. https://doi.org/10.1016/j.jaap.2017.11.010.

Ohra-aho, T., Gomes, F.J.B., Colodette, J.L., Tamminen, T., 2013. S/G ratio and lignin structure among Eucalyptus hybrids determined by Py-GC/MS and nitrobenzene oxidation. J. Anal. Appl. Pyrolysis 101, 166–171. https://doi.org/10.1016/j.jaap.2013.01.015.

Ohra-aho, T., Tenkanen, M., Tamminen, T., 2005. Direct analysis of lignin and lignin-like components from softwood kraft pulp by Py-GC/MS techniques. J. Anal. Appl. Pyrolysis, Pyrolysis 2004 (74), 123–128. https://doi.org/10.1016/j.jaap.2004.11.010.

Oudiani, A.E., Chaabouni, Y., Msahli, S., Sakli, F., 2011. Crystal transition from cellulose I to cellulose II in NaOH treated Agave americana L. fibre. Carbohydr. Polym. 86, 1221–1229. https://doi.org/10.1016/j.carbpol.2011.06.037.

Peng, Y., Wu, S., 2010. The structural and thermal characteristics of wheat straw hemicellulose. J. Anal. Appl. Pyrolysis 88, 134–139. https://doi.org/10.1016/j.jaap.2010.03.006.

Piskorz, J., Radlein, D., Scott, D.S., 1986. On the mechanism of the rapid pyrolysis of cellulose. J. Anal. Appl. Pyrolysis 9, 121–137. https://doi.org/10.1016/0165-2370(86)85003-3.

Ponder, G.R., Richards, G.N., 1991. Thermal synthesis and pyrolysis of a xylan. Carbohydr. Res. 218, 143–155. https://doi.org/10.1016/0008-6215(91)84093-T.

Prins, M.J., Ptasinski, K.J., Janssen, F.J.J.G., 2006a. Torrefaction of wood. Part 2. Anal. Prod. J. Anal. Appl. Pyrolysis 77, 35–40. https://doi.org/10.1016/j.jaap.2006.01.001.

Prins, M.J., Ptasinski, K.J., Janssen, F.J.J.G., 2006b. Torrefaction of wood: Part 1. Weight Loss Kinet. J. Anal. Appl. Pyrolysis 77, 28–34. https://doi.org/10.1016/j.jaap.2006.01.002.

Rodriguez Alonso, E., 2015. Contribution to the study of formation mechanisms of condensable by-products from torrefaction of various biomasses. Toulouse, INPT.

Rodriguez Alonso, E., Dupont, C., Heux, L., Da Silva Perez, D., Commandre, J.-M., Gourdon, C., 2016. Study of solid chemical evolution in torrefaction of different biomasses through solid-state 13C cross-polarization/magic angle spinning NMR (nuclear magnetic resonance) and TGA (thermogravimetric analysis). Energy 97, 381–390. https://doi.org/10.1016/j.energy.2015.12.120.

Saldarriaga, J.F., Aguado, R., Pablos, A., Amutio, M., Olazar, M., Bilbao, J., 2015. Fast characterization of biomass fuels by thermogravimetric analysis (TGA). Fuel 140, 744–751. https://doi.org/10.1016/j.fuel.2014.10.024.

Scheirs, J., Camino, G., Tumiatti, W., 2001. Overview of water evolution during the thermal degradation of cellulose. Eur. Polym. J. 37, 933–942. https://doi.org/10.1016/S0014-3057(00)00211-1.

Scheller, H.V., Ulvskov, P., 2010. Hemicelluloses. Annu. Rev. Plant Biol. 61, 263–289. https://doi.org/10.1146/annurev-arplant-042809-112315.

Shafizadeh, F., McGinnis, G.D., Philpot, C.W., 1972. Thermal degradation of xylan and related model compounds. Carbohydr. Res. 25, 23–33. https://doi.org/10.1016/S0008-6215(00)82742-1.

Shen, D.K., Gu, S., 2009. The mechanism for thermal decomposition of cellulose and its main products. Bioresour. Technol. 100, 6496–6504. https://doi.org/10.1016/j.biortech.2009.06.095.

Shen, D.K., Gu, S., Bridgwater, A.V., 2010a. Study on the pyrolytic behaviour of xylan-based hemicellulose using TG–FTIR and Py–GC–FTIR. J. Anal. Appl. Pyrolysis 87, 199–206. https://doi.org/10.1016/j.jaap.2009.12.001.

Shen, D.K., Gu, S., Bridgwater, A.V., 2010b. The thermal performance of the polysaccharides extracted from hardwood: cellulose and hemicellulose. Carbohydr. Polym. 82, 39–45. https://doi.org/10.1016/j.carbpol.2010.04.018.

Shen, D.K., Gu, S., Luo, K.H., Wang, S.R., Fang, M.X., 2010c. The pyrolytic degradation of wood-derived lignin from pulping process. Bioresour. Technol. 101, 6136–6146. https://doi.org/10.1016/j.biortech.2010.02.078.

Stefanidis, S.D., Kalogiannis, K.G., Iliopoulou, E.F., Michailof, C.M., Pilavachi, P.A., Lappas, A.A., 2014. A study of lignocellulosic biomass pyrolysis via the pyrolysis of cellulose, hemicellulose and lignin. J. Anal. Appl. Pyrolysis 105, 143–150. https://doi.org/10.1016/j.jaap.2013.10.013.

Tamminen, T., Campargue, M., Da Silva Perez, D., Dupont, C., Englund, F., Kotli, P., Larsson, S., Papadopoulou, E., Rasa, K., Raussi, T., Sajet, P., Wallin, M., 2016. Mobile and Flexible Processing of Biomass −EU project MOBILE FLIP.

Trubetskaya, A., Johnson, R., Monaghan, R.F.D., Ramos, A.S., Brunsvik, A., Wittgens, B., Han, Y., Pisano, I., Leahy, J.J., Budarin, V., 2021. Combined analytical strategies for chemical and physical characterization of tar from torrefaction of olive stone. Fuel 291, 120086. https://doi.org/10.1016/j.fuel.2020.120086.

Wang, S., Dai, G., Ru, B., Zhao, Y., Wang, X., Zhou, J., Luo, Z., Cen, K., 2016. Effects of torrefaction on hemicellulose structural characteristics and pyrolysis behaviors. Bioresour. Technol. 218, 1106–1114. https://doi.org/10.1016/j.biortech.2016.07.075.

Wang, S., Guo, X., Liang, T., Zhou, Y., Luo, Z., 2012. Mechanism research on cellulose pyrolysis by Py-GC/MS and subsequent density functional theory studies. Bioresour. Technol. 104, 722–728. https://doi.org/10.1016/j.biortech.2011.10.078.

Wang, Z., McDonald, A.G., Westerhof, R.J.M., Kersten, S.R.A., Cuba-Torres, C.M., Ha, S., Pecha, B., Garcia-Perez, M., 2013. Effect of cellulose crystallinity on the formation of a liquid intermediate and on product distribution during pyrolysis. J. Anal. Appl. Pyrolysis 100, 56–66. https://doi.org/10.1016/j.jaap.2012.11.017.

Werner, K., Pommer, L., Broström, M., 2014. Thermal decomposition of hemicelluloses. J. Anal. Appl. Pyrolysis 110, 130–137. https://doi.org/10.1016/j.jaap.2014.08.013.

Williams, P.T., Besler, S., 1996. The influence of temperature and heating rate on the slow pyrolysis of biomass. Renew. Energy 7, 233–250. https://doi.org/10.1016/0960-1481(96)00006-7.

Worasuwannarak, N., Sonobe, T., Tanthapanichakoon, W., 2007. Pyrolysis behaviors of rice straw, rice husk, and corncob by TG-MS technique. J. Anal. Appl. Pyrolysis 78, 265–271. https://doi.org/10.1016/j.jaap.2006.08.002.

Wu, Y., Zhao, Z., Li, H., He, F., 2009. Low temperature pyrolysis characteristics of major components of biomass. J. Fuel Chem. Technol. 37, 427–432. https://doi.org/10.1016/S1872-5813(10)60002-3.

Yang, H., Yan, R., Chen, H., Lee, D.H., Zheng, C., 2007. Characteristics of hemicellulose, cellulose and lignin pyrolysis. Fuel 86, 1781–1788. https://doi.org/10.1016/j.fuel.2006.12.013.

Zhang, J., Luo, J., Tong, D., Zhu, L., Dong, L., Hu, C., 2010. The dependence of pyrolysis behavior on the crystal state of cellulose. Carbohydr. Polym. 79, 164–169. https://doi.org/10.1016/j.carbpol.2009.07.038.

Zhang, S., Su, Y., Ding, K., Zhu, S., Zhang, H., Liu, X., Xiong, Y., 2018. Effect of inorganic species on torrefaction process and product properties of rice husk. Bioresour. Technol. 265, 450–455. https://doi.org/10.1016/j.biortech.2018.06.042.

Zhao, C., Jiang, E., Chen, A., 2017. Volatile production from pyrolysis of cellulose, hemicellulose and lignin. J. Energy Inst. 90, 902–913. https://doi.org/10.1016/j.joei.2016.08.004.

Zhao, J., Xiuwen, W., Hu, J., Liu, Q., Shen, D., Xiao, R., 2014. Thermal degradation of softwood lignin and hardwood lignin by TG-FTIR and Py-GC/MS. Polym. Degrad. Stab. 108, 133–138. https://doi.org/10.1016/j.polymdegradstab.2014.06.006.